
Investigation of the modulation
of murine repeat element DNA
methylation by ionising radiation
in vivo

A thesis submitted in fulfilment for the degree of Doctor of Philosophy

Michelle Renee Newman, B.Sc, B.HSc (Hons)

Haematology and Genetic Pathology

School of Medicine, Faculty of Health Sciences

Flinders University

November 2012

TABLE OF CONTENTS

TABLE OF CONTENTS	I
FIGURES	VIII
TABLES	XII
SUMMARY	XIV
DECLARATION	XVIII
ACKNOWLEDGEMENTS.....	XIX
ABBREVIATIONS AND UNITS OF MEASUREMENT	XXII
<i>STANDARD INTERNATIONAL UNITS OF MEASURE</i>	<i>XXIV</i>
<i>INDICATORS OF MAGNITUDE.....</i>	<i>XXIV</i>
PUBLICATIONS AND PRESENTATIONS ARISING FROM THIS THESIS	XXV
PUBLICATIONS	XXV
PRESENTATIONS.....	XXV
1 INTRODUCTION	1
1.1 IONISING RADIATION	3
1.1.1 <i>Quantifying ionising radiation.....</i>	<i>4</i>
1.2 BIOLOGICAL EFFECTS OF RADIATION.....	6
1.2.1 <i>Mouse models in radiation research.....</i>	<i>6</i>
1.2.2 <i>High dose radiation exposure.....</i>	<i>9</i>
1.2.2.1 Tissue effects from high dose radiation exposure	9
1.2.2.2 Sub-cellular effects from high dose radiation exposure	10
1.2.2.3 Repair of DNA following high dose radiation exposure	13
1.2.3 <i>Low dose radiation exposure</i>	<i>14</i>
1.2.4 <i>Ageing and radiation exposure</i>	<i>16</i>
1.3 MAINTENANCE OF GENOMIC STABILITY	17
1.3.1 <i>Chromatin structure</i>	<i>17</i>
1.3.2 <i>DNA methylation.....</i>	<i>21</i>

1.3.2.1	Methods for the detection of DNA methylation.....	24
1.3.3	<i>Telomeres and genomic stability</i>	30
1.3.4	<i>Retrotransposons and genomic stability</i>	33
1.4	DNA METHYLATION AND RADIATION EXPOSURE.....	39
1.5	AIMS OF THIS THESIS.....	44
2	MATERIALS AND METHODS.....	45
2.1	MOUSE STRAINS.....	45
2.2	A11 CELL LINE.....	46
2.3	RADIATION DOSIMETRY AND X-IRRADIATION OF MICE.....	46
2.4	MOUSE TISSUES.....	48
2.4.1	<i>Mouse tissue isolation</i>	48
2.4.2	<i>Isolation of peripheral blood</i>	48
2.5	ANALYSIS OF DNA METHYLATION.....	49
2.5.1	<i>Extraction of genomic DNA</i>	49
2.5.2	<i>Bisulphite modification of genomic DNA</i>	50
2.5.3	<i>Primer design</i>	51
2.5.4	<i>PCR and high resolution melt analysis (HRM)</i>	51
2.5.5	<i>Calculation of the Net Temperature Shift</i>	52
2.5.6	<i>Gel electrophoresis of PCR products</i>	52
2.5.7	<i>Sequence analysis of PCR products</i>	53
2.5.7.1	Sanger sequencing.....	53
2.5.7.2	Pyrosequencing.....	53
2.5.8	<i>Liquid chromatography-Mass spectrometry (LC-MS)</i>	54
2.5.8.1	DNA hydrolysis.....	54
2.5.8.2	LC-MS Procedure.....	54
2.6	TELOMERE LENGTH ANALYSIS.....	55
2.7	L1 TRANSCRIPT ANALYSIS.....	56
2.7.1	<i>RNA extraction</i>	56
2.7.1.1	RNA quality control.....	57
2.7.1.2	DNaseI treatment.....	57
2.7.2	<i>Reverse transcription</i>	58

2.7.3	<i>Quantitative real-time PCR</i>	58
2.7.3.1	Primer design	59
2.7.3.2	Analysis of reference gene stability	59
2.8	WESTERN BLOT ANALYSIS	59
2.8.1	<i>Acid extraction of histone proteins</i>	59
2.8.2	<i>Determination of protein concentration</i>	60
2.8.3	<i>Gel Electrophoresis of protein lysates</i>	61
2.8.4	<i>Semi-dry transfer of proteins</i>	62
2.8.5	<i>Detection of proteins</i>	62
2.8.5.1	Antibody detection of proteins.....	62
2.8.5.2	Quantitation of protein bands	63
2.9	IMMUNOHISTOCHEMISTRY	63
2.9.1	<i>Preparation of tissue sections</i>	63
2.9.2	<i>Detection of spleen T-cells</i>	63
2.9.3	<i>Microscopy of spleen sections</i>	64
2.10	STATISTICAL ANALYSIS.....	65
3	DEVELOPMENT AND VALIDATION OF A MURINE LINE1 DNA METHYLATION HIGH RESOLUTION MELT ASSAY	66
3.1	RESULTS.....	69
3.1.1	<i>Design of a murine L1 repeat element high resolution melt assay</i>	69
3.1.1.1	Identification of murine LINE1 repeat element	69
3.1.1.2	Primer Design.....	69
3.1.1.3	Sequence analysis of LINE1 repeat elements	70
3.1.1.4	Development of PCR methylation controls.....	72
3.1.1.5	High resolution melt analysis of control DNA	73
3.1.2	<i>Detection of demethylation using the L1-HRM assay</i>	74
3.1.2.1	Detection of demethylation induced by 5-aza treatment	74
3.1.2.2	Biasing of PCR primers to enhance sensitivity	77
3.1.2.3	Statistical analysis of methylation differences between samples using the Net Temperature Shift.....	79
3.1.3	<i>Validation of L1-HRM assay</i>	80

3.1.3.1	Pyrosequencing	80
3.1.3.2	Liquid chromatography-mass spectrometry	82
3.1.3.3	Sensitivity, reproducibility and linearity of the L1-HRM assay	84
3.1.4	<i>Application of the HRM methylation assay to other murine repeat elements</i>	87
3.1.4.1	SINE1 and IAP_LTR repeat elements	87
3.2	DISCUSSION	89
3.2.1	<i>Detection of demethylation using the L1-HRM assay</i>	89
3.2.2	<i>Validation of HRM assay detection of methylation differences</i>	92
3.2.3	<i>Reproducibility, sensitivity and linearity of the L1-HRM assay</i>	94
3.2.4	<i>Conclusion</i>	96
4	ANALYSIS OF REPEAT ELEMENT DNA METHYLATION CHANGES IN MOUSE STRAINS WITH DIFFERING RADIATION SENSITIVITIES FOLLOWING EXPOSURE TO IONISING RADIATION	97
4.1	RESULTS	99
4.1.1	<i>L1 methylation levels in mouse spleen 6-7 days following 1 Gy X-irradiation</i>	99
4.1.1.1	Pyrosequencing analysis of spleen L1-HRM assay samples from male BALB/c and female CBA mice 6 days following 1 Gy X-irradiation	101
4.1.2	<i>LC-MS analysis of male BALB/c and female CBA mouse spleen total genomic DNA methylation levels 6 days following 1 Gy X-irradiation</i> ...	104
4.1.3	<i>B1 and IAP repeat element methylation levels of male and female BALB/c and CBA mouse spleen 6 days following 1 Gy X-irradiation</i>	105
4.1.4	<i>Analysis of temporal spleen methylation changes in C57Bl/6 mice following 1 Gy X-irradiation</i>	106
4.1.4.1	Pyrosequencing analysis of spleen L1 methylation changes in C57Bl/6 mice 1 and 14 days following 1 Gy X-irradiation	107
4.1.4.2	LC-MS analysis of spleen tissue genomic DNA from C57Bl/6 mice 1 and 14 days following 1 Gy X-irradiation	109
4.1.4.3	Spleen B1 and IAP element methylation levels in C57Bl/6 mice 14 days following 1 Gy X-irradiation	110

4.1.4.4	Pyrosequencing analysis of the methylation changes at all CpGs within the L1-HRM assay target sequence in the spleens of C57Bl/6 mice 14 days following 1 Gy X-irradiation	111
4.1.4.5	L1 promoter analysis.....	114
4.1.4.6	Analysis of histone H3 tri-methylation in the spleens of C57Bl/6 mice 14 days following 1 Gy X-irradiation	119
4.1.5	<i>Analysis of spleen temporal L1 methylation changes in BALB/c and CBA mice following 1 Gy X-irradiation</i>	<i>121</i>
4.1.6	<i>Tissue L1 methylation levels of untreated BALB/c, CBA and C57Bl/6 mice</i>	<i>123</i>
4.1.7	<i>Tissue responses 6 days following 1 Gy X-irradiation in male and female BALB/c and CBA mice</i>	<i>126</i>
4.1.8	<i>Immunohistochemical analysis of spleen tissue cell populations</i>	<i>127</i>
4.2	DISCUSSION	133
4.2.1	<i>Strain differences in response to irradiation</i>	<i>133</i>
4.2.2	<i>Sex differences in L1 methylation levels in response to X-irradiation.....</i>	<i>142</i>
4.2.3	<i>Analysis of the effect of changes in methylation to the L1 promoter.....</i>	<i>143</i>
4.3	CONCLUSION.....	147
5	LONGITUDINAL STUDY OF REPEAT ELEMENT METHYLATION IN PERIPHERAL BLOOD IN RESPONSE TO LOW DOSE RADIATION.....	148
5.1	RESULTS.....	150
5.1.1	<i>Longitudinal study of repeat element DNA methylation in mice up to 299 days following 10 mGy X-irradiation (Longitudinal Study #1)</i>	<i>150</i>
5.1.1.1	Outline of study	150
5.1.1.2	Analysis of mouse weight and repeat element methylation changes following 10 mGy X- irradiation.....	151
5.1.2	<i>Longitudinal study of repeat element DNA methylation in mice up to 420 days following 10 mGy X-irradiation (Longitudinal Study #2)</i>	<i>159</i>
5.1.2.1	Outline of longitudinal study #2	159
5.1.2.2	Weight changes of male and female mice over time	160

5.1.2.3	Analysis of the effect of irradiation and ageing on peripheral blood genomic DNA up to 420 days following irradiation with 10 mGy X-rays.....	162
5.1.2.4	Analysis of the effect of 10 mGy X-irradiation and ageing on spleen genomic DNA from mice at 420 days post-irradiation	169
5.2	DISCUSSION	172
5.2.1	<i>Analysis of variation in NTS between PCRs</i>	172
5.2.2	<i>The longitudinal effect of 10 mGy X-irradiation on telomere length and repeat element methylation in spleen and peripheral blood up to 420 days post-irradiation</i>	175
5.3	CONCLUSION.....	182
6	GENERAL DISCUSSION.....	184
	REFERENCES.....	191
	APPENDIX A: ANALYSIS OF THE EFFECT OF C57BL/6-PKZ1 TRANSGENIC STATUS ON NTS	233
	APPENDIX B: PCR PRIMERS.....	234
	HRM PRIMERS.....	234
	<i>KATO</i>	234
	<i>LINE1</i>	234
	<i>B1_MM.....</i>	235
	<i>IAP_LTR</i>	235
	SEQUENCING PRIMERS.....	235
	QRT-PCR PRIMERS.....	236
	<i>L1-ORF1.....</i>	236
	<i>L1-ORF2.....</i>	236
	<i>COCH (COAGULATION FACTOR C HOMOLOGUE)</i>	236
	<i>CPB1 (CARBOXYPEPTIDASE B1).....</i>	237
	<i>GAPDH (GLYCERALDEHYDE-3-PHOSPHATE DEHYDROGENASE)</i>	237
	<i>PNLIP (PANCREATIC TRIACYLGLYCEROL LIPASE)</i>	237
	<i>POLR2C (POLYMERASE (RNA) II (DNA DIRECTED) POLYPEPTIDE C)</i>	238
	<i>RN18S (RIBONUCLEOTIDE PROTEIN SUBUNIT 18).....</i>	238
	<i>SPI-C (TRANSCRIPTION FACTOR SPI-C)</i>	238
	TELOMERE ASSAY PRIMERS	239

<i>TELOMERE</i>	239
TELOMERE OLIGONUCLEOTIDE STANDARD	239
<i>36B4 (LARGE RIBOSOMAL PROTEIN, PO)</i>	239
<i>36B4</i> OLIGONUCLEOTIDE STANDARD	239
APPENDIX C: SOLUTIONS AND BUFFERS.....	240
AGAROSE GEL ELECTROPHORESIS	240
0.5 X TRIS-BORATE EDTA (TBE) BUFFER	240
2% AGAROSE GEL	240
6 X FICOLL LOADING BUFFER.....	240
WESTERN BLOT.....	240
HISTONE LYSIS BUFFER.....	240
TRIS-EDTA	241
1 X RUNNING BUFFER	241
4 X LOADING BUFFER.....	241
1 X TRANSFER BUFFER	241
10 X TRIS BUFFERED SOLUTION (TBS).....	242
1 X TBS-TWEEN (TBS-T)	242
IMMUNOHISTOCHEMISTRY.....	242
APES SOLUTION	242
2% FORMALDEHYDE.....	242
BLOCKING SOLUTION	242
APPENDIX D: L1 PROMOTER AND ORF SEQUENCES.....	243
APPENDIX E: TELOMERE LENGTH AND GENOME COPY NUMBER	
CALCULATIONS	246
CALCULATION OF TELOMERE LENGTH	246
TELOMERE OLIGONUCLEOTIDE STANDARDS	247
CALCULATION OF GENOME COPY NUMBER.....	247
<i>36B4</i> OLIGONUCLEOTIDE STANDARDS	248
TELOMERE LENGTHS OF MICE FROM LONGITUDINAL STUDY OF METHYLATION IN PB IN RESPONSE TO LOW DOSE RADIATION.....	249
APPENDIX F: CELLPROFILER™ PIPELINE	250
APPENDIX G: PUBLICATIONS ARISING FROM THIS THESIS	251

FIGURES

Figure 1-1: Sources of radiation exposure.....	2
Figure 1-2: Linear no-threshold model.....	2
Figure 1-3: Measurement of radiation exposure.....	4
Figure 1-4: Tissue/organ radiation weighting factors.....	6
Figure 1-5: Damage to DNA following high dose radiation exposure.....	12
Figure 1-6: Control of chromatin structure by epigenetic modifications.....	19
Figure 1-7: Methylation of cytosine.....	22
Figure 1-8: Facilitation of mutations via demethylation of cytosine.....	24
Figure 1-9: Techniques that utilise bisulphite modification to evaluate methylation levels.....	26
Figure 1-10: Structure of telomeres.....	32
Figure 1-11: Types of retrotransposons.....	34
Figure 1-12: L1 transcription and retrotransposition.....	36
Figure 1-13: IAP transcription and retrotransposition.....	37
Figure 3-1: Agarose gel analysis of L1 PCR products.....	70
Figure 3-2: The L1 sequence confirmed by DNA sequencing.....	72
Figure 3-3: High resolution melt analysis of control DNA.....	74
Figure 3-4: Melt curve analysis of unmodified genomic DNA.....	76
Figure 3-5: Detection of 5-aza induced partial demethylation of murine L1 elements in A11 cells using methylation-status unbiased L1 primers.....	76
Figure 3-6: Detection of 5-aza induced partial demethylation of murine L1 elements in A11 cells using unmethylated-biased L1 primers.....	78
Figure 3-7: Quantitation of methylation differences using the Net Temperature Shift.....	80
Figure 3-8: Schematic diagram of the L1 pyrosequencing target sequence.....	81
Figure 3-9: Pyrosequencing of 5-aza treated A11 cells L1-HRM PCR products.....	82
Figure 3-10: Analysis of total genomic 5mdC content in 5-aza treated A11 cells.....	83
Figure 3-11: Linearity of L1-HRM assay.....	85

Figure 3-12: Murine B1 and Intracisternal-A-Particle Long Terminal Repeat element sequences..... 88

Figure 3-13: Demethylation of B1 and IAP_LTR repeat elements after 5-aza treatment..... 88

Figure 4-1: Spleen tissue L1 methylation in BALB/c, CBA and C57Bl/6 mice 6-7 days following irradiation with 1 Gy X-rays..... 100

Figure 4-2: LC-MS and pyrosequencing analysis of spleen methylation levels in male BALB/c and female CBA mice 6 days following 1 Gy X-irradiation. 103

Figure 4-3: LC-MS analysis of total splenic genomic DNA methylation levels in male BALB/c and female CBA mice 6 days following 1 Gy X-irradiation. 104

Figure 4-4: B1 and IAP repeat element methylation in spleen tissues from BALB/c and CBA mice 6 days following 1 Gy X-irradiation..... 105

Figure 4-5: L1 methylation levels in C57Bl/6 spleen tissue up to 14 days following irradiation with 1 Gy X-rays..... 107

Figure 4-6: Pyrosequencing analysis of spleen methylation levels from C57Bl/6 mice 1 and 14 days following irradiation with 1 Gy X-rays..... 108

Figure 4-7: LC-MS analysis of spleen genomic 5mdC levels from C57Bl/6 mice 14 days following irradiation with 1 Gy X-rays..... 109

Figure 4-8: C57Bl/6 mouse spleen tissue B1 and IAP element methylation 14 days following irradiation with 1 Gy X-rays..... 110

Figure 4-9: L1 pyrosequencing dispensation sequence..... 112

Figure 4-10: Pyrosequencing analysis of all CpGs within the L1 CpG island of spleen samples from C57Bl/6 mice 14 days following irradiation with 1 Gy X-rays..... 113

Figure 4-11: Analysis of the L1 promoter sequence..... 116

Figure 4-12: L1 transcript levels in the spleen tissues of C57Bl/6 mice 14 days following irradiation with sham or 1 Gy X-rays..... 118

Figure 4-13: L1 transcript expression in 5-aza treated A11 cells..... 119

Figure 4-14: Analysis of histone H3 tri-methylation in spleen tissue of C57Bl/6 mice 14 days following 1 Gy X-irradiation..... 120

Figure 4-15: BALB/c and CBA L1 methylation levels 1, 6 and 14 days following irradiation with 1 Gy X-rays..... 122

Figure 4-16: L1 methylation in various tissues from the BALB/c, CBA and C57Bl/6 mouse strains..... 124

Figure 4-17: Analysis of male BALB/c tissue panel with methylation-status unbiased L1 primers. 125

Figure 4-18: Detection of splenic T-cells in male BALB/c and CBA mice using immunohistochemistry. 128

Figure 4-19: CellProfiler™ identification of splenic T-cells. 130

Figure 4-20: The roving mean of T-cell areas in BALB/c spleen..... 131

Figure 4-21: Mean splenic T-cell staining area frequency of male BALB/c and CBA mice. 132

Figure 4-22: Correlation of NTS and splenic T-cell area frequency. 132

Figure 5-1: Outline of longitudinal study..... 150

Figure 5-2: Mean weight over time of mice irradiated with sham and 10 mGy X-rays up to 299 days post-irradiation. 152

Figure 5-3: Outline of sample randomisation for HRM analysis..... 153

Figure 5-4: Mean PB L1 NTS of mice up to 85 days post-irradiation with 10 mGy X-rays. 154

Figure 5-5: PB L1 and B1 element NTS of mice up to 299 days post-irradiation with sham or 10 mGy X-rays. 155

Figure 5-6: Mean L1 and B1 element NTS of PB samples up to 299 days following irradiation with sham or 10 mGy X-rays. 157

Figure 5-7: Spleen NTS of L1 and B1 elements from mice 299 days post-irradiation with sham and 10 mGy X-rays..... 158

Figure 5-8: Outline of second longitudinal study. 159

Figure 5-9: Mean weight over time for male and female mice irradiated with sham and 10 mGy X-rays. 161

Figure 5-10: Telomere length of individual male and female mice pre- and post-irradiation with 10 mGy X-rays. 163

Figure 5-11: Mean telomere length of male and female mice pre- and post-irradiation with 10 mGy X-rays.	164
Figure 5-12: PB NTS for L1 and B1 elements for mice up to 420 days post-irradiation with sham or 10 mGy X-rays.	166
Figure 5-13: Mean PB NTS for L1 and B1 elements from mice up to 420 days post-irradiation with sham or 10 mGy X-rays.	168
Figure 5-14: Correlation of L1 and B1 element NTS for PB.....	169
Figure 5-15: Analysis of spleen telomere length at 420 days post-irradiation with sham or 10 mGy X-rays compared to young untreated mice.	170
Figure 5-16: Spleen L1 NTS of mice 420 days post-irradiation compared with untreated young mice and analysis of B1 element NTS of mice 420 days post-irradiation with sham and 10 mGy X-rays.....	171

TABLES

Table 1: LD _{50:30} of inbred mouse strains following single whole body X-irradiation.....	8
Table 2: Days survival following daily whole-body X-irradiation with 10 Gy of the C57Bl/6, BALB/c and CBA mouse strains in a study of twenty-seven mouse strains.	9
Table 3: Number of events of the different types of DNA damage that can occur in a cell following irradiation with 1 Gy X-rays.	13
Table 4: Summary of published <i>in vivo</i> murine DNA methylation and ionising radiation studies.	41
Table 5: Summary of published <i>in vivo</i> transgenerational murine DNA methylation and ionising radiation studies.	42
Table 6: Dosimetry parameters for irradiation experiments.....	48
Table 7: Frequency of sequence variants detected at 10 nucleotide positions in the L1-HRM target sequence.....	71
Table 8: Analysis of variability of L1-HRM assay.....	86
Table 9: Pearson correlation of L1, B1 and IAP repeat element NTS values for the 5-aza treated A11 cell line samples.	89
Table 10: L1 CpG methylation levels (%) for male BALB/c and female CBA mice 6 days following 1 Gy X-irradiation using pyrosequencing.....	102
Table 11: Correlation of L1 transcript levels with LC-MS and pyrosequencing mean methylation.	118
Table 12: Mean L1 NTS for tissues from BALB/c and CBA mice treated with 1 Gy X-rays.....	126
Table 13: Mean L1 NTS for peripheral blood samples from BALB/c and CBA mice treated with 1 Gy X-rays.....	127
Table 14: Age of mice at PB sampling in longitudinal study (#1) up to 299 days post-irradiation with 10 mGy X-rays.	151
Table 15: Analysis of changes in PB L1 and B1 element NTS up to 299 days following irradiation with 10 mGy X-rays.....	156

Table 16: Age of mice at PB sampling in longitudinal study (#2) up to 420 days post-irradiation with 10 mGy X-rays.	160
Table 17: Analysis of changes in mouse weight up to 420 days post-irradiation with 10 mGy X-rays.	161
Table 18: Analysis of changes in PB L1 and B1 repeat element NTS in male and female mice up to 420 days post-irradiation with 10 mGy X-rays.	167
Table 19: Mean difference in L1 NTS between bisulphite modification and PCR groups for PB samples up to 85 days post-irradiation amplified with the unmethylated-biased primers.	173
Table 20: Comparison of the mean L1 NTS for three PCR groups from longitudinal study #2 amplified with the methylation status-unbiased primers.	174
Table 21: Independent samples T-test analysis of pKZ1-C57Bl/6 transgenic status.	233
Table 22: Telomere oligonucleotide standard lengths.	247
Table 23: 36B4 oligonucleotide standard copy numbers.	248
Table 24: Mean length per telomere of PB samples from Chapter 5 (Section 5.1.2.3.1).	249
Table 25: Mean length per telomere of spleen samples from Chapter 5 (Section 5.1.2.4.1).	249

SUMMARY

Mouse models that are used to investigate the biological effects of ionising radiation exposure have shown that different inbred strains respond differently to radiation exposure. Based on end-points such as time to lethality, repair of DNA damage and the development of cancers, these strains are defined as radiation-sensitive or resistant. Ionising radiation has been reported to induce a loss of DNA methylation, a modification of cytosine residues (predominantly when in sequence with a guanine; termed a CpG) that plays an important role in maintaining genome stability by influencing the expression of genes through chromatin structure. The most heavily methylated regions of the genome are found at transposable repeat elements, where a loss of methylation may result in transposition and increased genomic instability. It is not known whether the radiation sensitivity that these animals exhibit is influenced by the modulation of DNA methylation by ionising radiation. This thesis describes the investigation of the modulation of DNA methylation of a class of repeat elements known as LINE1 (L1), in three strains of laboratory mice that differ in radiosensitivity: the C57Bl/6 (radiation-resistant), BALB/c and CBA (radiation-sensitive) mouse strains. A sensitive PCR-based assay was developed in order to investigate the changes in L1 methylation following radiation exposure. The L1 assay utilised high resolution melt technology (HRM), which is able to distinguish between single nucleotide differences in sequences of DNA following PCR amplification. The L1-HRM assay was demonstrated to be able to detect differences in heterogeneous CpG methylation as small as 3%; and was also able to detect changes in methylation between samples that could not be

detected by the gold standard method for total genomic 5mdC quantitation (liquid chromatography mass-spectrometry). Compared with other PCR-based methods for DNA methylation analysis, the L1-HRM assay was shown to be a sensitive, high through-put screening tool that did not require post-PCR manipulation in order to detect differences in methylation between samples.

Following high dose irradiation (1 Gy), the radiosensitive mouse strains (BALB/c and CBA) exhibited early increases in spleen L1 methylation, which had returned to sham methylation levels by 14 days following irradiation. Differences in responses between male and female mice were also observed, with the male CBA mice demonstrating an earlier response in comparison with the female CBA mice. The radiation-resistant C57Bl/6 mice demonstrated a late change in methylation, where a loss of methylation was observed by 14 days following irradiation. The modulation of L1 DNA methylation was shown to only affect some CpGs within the L1-HRM assay target region, which was consistent across the three strains. This is the first analysis of the modulation of murine L1 element CpGs following radiation exposure. Furthermore, the loss of methylation in the C57Bl/6 mice did not result in an increase in L1 element transcripts. Other murine repeat DNA elements (B1 and Intracisternal-A particle long terminal repeat elements) were found to display similar modulation to that of the L1 elements following irradiation. These results show that strains that differ in radiosensitivity exhibit temporal differences in repeat element methylation responses following exposure to ionising radiation, highlighting the importance of timing of analysis, particularly when analysing the effects of a modulator of DNA methylation that does not appear to affect every

CpG. This is the first direct comparison of the temporal DNA methylation response of three strains of mice that differ in radiosensitivity.

Low doses of ionising radiation have been shown to demonstrate a protective role for endpoints such as DNA damage and tumour progression, termed the radioadaptive response. The exact mechanism(s) involved in the radioadaptive response are still being identified, and it has been suggested that stabilisation of the genome via the modulation of DNA methylation may be involved. Both radiation exposure and ageing are associated with increased genomic instability, shorter telomeres and reduced DNA methylation. Studies described in this thesis investigated whether a low dose radiation (10 mGy) exposure would modulate repeat element DNA methylation to induce an adaptive response. Following irradiation, the modulation of L1 and B1 DNA methylation of ageing mice was monitored over time using peripheral blood (PB) sampling. A decline in PB L1 and B1 element methylation levels was not observed by 420 days (~18 months of age) post-irradiation; however spleen L1 methylation levels increased with age. No effect of irradiation was detected on PB and spleen L1 and B1 methylation levels or telomere length in the ageing mice. These results indicate that there may be an age-threshold at which repeat element methylation levels decline in ageing animals. Furthermore, these results suggest that a low dose ionising radiation exposure does not elicit a long term effect on DNA methylation levels, nor is an adaptive response induced. This is the first study of the long term effect of a low dose ionising radiation exposure on DNA methylation levels.

Very little is known about the effect of radiation exposure on repeat element DNA methylation at the doses used in this thesis. This is the first *in vivo* methylation study to use low doses of radiation that are in the adaptive response range. The results obtained using the L1-HRM assay exemplify the dynamic nature of DNA methylation over time, both in ageing animals and in response to ionising radiation exposure, highlighting the importance of timing of analysis, tissue type and age of an animal when interpreting DNA methylation responses to exogenous agents.

DECLARATION

I certify that this thesis does not incorporate without acknowledgment any material previously submitted for a degree or diploma in any university; and that to the best of my knowledge and belief it does not contain any material previously published or written by another person except where due reference is made in the text.

Michelle Renee Newman

ACKNOWLEDGEMENTS

First and foremost I would like to thank Professor Pam Sykes for giving me the opportunity to undertake a PhD in her laboratory. It is always a gamble to take on a new student, more so when that student was a research assistant for a number of years and has many habits to break! I would also like to thank Pam for providing me with the opportunities that I have had during my PhD to advance my scientific career and help me grow as a scientist. Furthermore, I would not have been able to undertake my PhD if it were not for the scholarship provided by the Flinders Medical Centre Foundation and BHP Billiton.

Special thanks to my co-supervisor Dr Rebecca Ormsby. Thank you for your support, both with useful discussions, suggestions, countless hours of proof-reading, and friendship throughout my time here.

Most of the work described in this thesis was performed using mice. These experiments involved numerous irradiation experiments for which I would like to thank Associate Professor Eva Bezak for donating her time to perform the irradiations, calculation of the dosimetry, as well as undertaking some proof-reading. I am extremely grateful to have had the opportunity to have her involved in my research.

For their help with the mice used during the course of this study I thank the Flinders University School of Medicine Animal Facility.

The work from this thesis could not have been performed if it were not for the hours of time donated by both past and present members of the Sykes' lab. A big thankyou in no particular order goes to Dr Rebecca Ormsby, Mark Lawrence, Dr Benjamin Blyth, Dr Alex Staudacher, Ami Cochrane, Anzhen Jian, Katrina Bexis, Katherine Tulloch and Cameron Dougherty. I would also like to thank Dr Tanya Day, whose archival tissue culture experiments were used in this thesis.

Thanks also, to Dr Damian Hussey and Dr George Mayne for their help in the initial optimisation of the HRM assay; Dr Daniel Jardine for performing the LC-MS, and Dr Peta Macardle for useful discussion regarding the immunohistochemistry.

I would also like to thank the Low Dose Radiation Research Program, Biological and Environmental Research, U.S. Department of Energy for funding; and to Flinders University, the Flinders Medical Centre Volunteers Service, the Australian Radiation Protection Society and the Australian Institute of Nuclear Science and Engineering for providing funding to attend national and international conferences.

Personally, I would like to thank Dr Tina Bianco-Miotto, who unintentionally became a mentor, and encouraged me to take the big step to undertake a PhD. Thanks also to Tania Pfeiffer, whose regular coffee visits, especially during writing-up, were a much needed and welcomed break! I would like to thank my family and friends for their support over the years. Many of you were probably questioning my sanity at

times. In particular I would like to thank my mum, Monique, Carly, Steph and Jane for their support. Also to Em, Jase and James for the much needed climbing time.

Finally, a big thank you, hugs and kisses to Layla, Drew, Curtis and Zoe. Without you, life would have been boring and far too serious. Your smiles and giggles made the hard times easy to bear. You are the best nieces' and nephew anyone could ask for and I love you all to bits.

ABBREVIATIONS AND UNITS OF MEASUREMENT

A	amp
APES	aminopropylethoxysilane
5-aza	5-aza-2'-deoxycytidine
bp	base pair
BSA	bovine serum albumin
cDNA	complementary DNA
DAPI	4, 6-diamidino-2-phenylindole
DNA	deoxyribonucleic acid
DSB	double strand breaks
dsDNA	double-stranded DNA
DMSO	dimethyl sulphoxide
DNMT	DNA methyltransferase
DTT	dithiothreitol
FITC	fluorescein isothiocyanate
<i>g</i>	relative centrifugal force
gDNA	genomic DNA
GI	genomic instability
HDR	high dose radiation
HPLC	high performance liquid-chromatography
HRM	high resolution melt
HVL	half value layer
IAP_LTR	intracisternal-A-particle long terminal repeat
kb	kilo base
LC-MS	liquid chromatography mass-spectrometry
LDR	low dose radiation
LET	linear energy transfer
LINE; L1	long interspersed nucleic elements

5mdC	5-methyl-deoxycytosine
MLT	mean length per telomere
NTS	net temperature shift
ORF	open reading frame
PB	peripheral blood
PBS	phosphate buffered saline
PVDF	polyvinylidene difluoride
ROS	reactive oxygen species
RNA	ribonucleic acid
qRT-PCR	quantitative real-time polymerase chain reaction
SINE	short interspersed nucleic elements
SSB	single strand breaks
ssDNA	single stranded DNA
T_m	melting temperature
V	volt
v/v	volume for volume
w/v	weight for volume

Standard international units of measure

°C	degree Celsius
g	gram
Gy	Gray
h	hour
d	day(s)
L	litre
M	Mole
min	minutes
s	seconds
Sv	Seivert

Indicators of magnitude

k	Kilo	(x 10 ³)
m	milli	(x 10 ⁻³)
μ	micro	(x 10 ⁻⁶)
n	nano	(x 10 ⁻⁹)

PUBLICATIONS AND PRESENTATIONS ARISING FROM THIS THESIS

Publications

Michelle R Newman, Benjamin J. Blyth, Damian J. Hussey, Daniel Jardine, Pamela J. Sykes and Rebecca J. Ormsby. (2012) Sensitive quantitative analysis of murine LINE1 DNA methylation using high resolution melt analysis. *Epigenetics*. 7(1): 92-101.

Presentations

M.R. Newman, B.J. Blyth, E. Bezak, P.J. Sykes and R.J. Ormsby. Analysis of LINE1 repeat element Methylation changes following high dose radiation exposure in C57Bl/6, BALB/c and CBA mice. 4th Australian Epigenetics Scientific Conference, 7-9th May, Adelaide, Australia 2012.

M.R. Newman, B.J. Blyth, E. Bezak, P.J. Sykes and R.J. Ormsby. Changes to global DNA methylation in three inbred mouse strains with differing radiation sensitivities. AINSE Radiation Conference, 15th – 17th February, Lucas Heights, 2012.

M.R. Newman, B.J. Blyth, E. Bezak, D. Hussey, P.J. Hussey, P.J. Sykes and R.J. Ormsby. The use of high resolution melt analysis to investigate radiation sensitivity and changes to global DNA methylation in various mouse strains. 6th Chromatin Structure and Function, 5th – 8th December, Aruba, 2011.

Sykes P.J., **Newman M.R.**, Ormsby R.J., Blyth B.J. and Bezak E. Global DNA Methylation Responses to Low Dose Radiation Exposure. 36th Annual Conference of the Australasian Radiation Protection Society, Melbourne, Australia. 16-19 October, 2011.

Sykes P.J., **Newman M.R.**, Blyth B.J. and Ormsby R.J. Global methylation responses to low dose exposure. 14th International Congress on Radiation Research, Warsaw, Poland, 28th August – 1st September, 2011.

Newman M.R., Ormsby R.J., Blyth B.J., Bezak E., and Sykes P.J. Global DNA methylation responses to low dose radiation exposure. The Engineering and Physical Sciences in Medicine and the Australian Biomedical Engineering Conference, Darwin, NT, 14th-18th August 2011.

Newman, M.R., Blyth, B.J., Bezak, E., Sykes, P.J., and Ormsby, R.J. Detecting changes in global DNA methylation levels *in vivo* following low dose ionizing radiation exposure. 56th Annual Radiation Research Society Meeting, Maui, Hawaii. 25th-29th September 2010.

Newman, M.R., Blyth, B.J., Bezak, E., Sykes, P.J., and Ormsby, R.J. Investigation of DNA methylation levels *in vivo* in response to low dose radiation exposure. ARPS SA student oral presentation competition, Adelaide, Australia. 22nd June 2010.

Newman, M.R., Blyth, B.J., Bezak, E., Sykes, P.J., and Ormsby, R.J. Investigating DNA methylation as a mechanism in the low dose radiation induced adaptive response. ASMR Scientific Meeting 2010, Adelaide, Australia. 9th June 2010.

Newman, M.R., Blyth, B.J., Sykes, P.J., and Ormsby, R.J. Quantitation of global DNA methylation levels in response to low dose radiation exposure using high resolution melt curve analysis. Epigenetics 2009 Australian Scientific Conference, Melbourne, Australia. 1st -3rd December 2009.

1 INTRODUCTION

Humans are continually exposed to natural background radiation. In Australia, the average total exposure to background radiation is 2 mSv per year and can include natural sources of radiation such as cosmic radiation, radioactive elements in the earth's crust producing radon gas, and naturally occurring radionuclides found in food and water. Exposure to radiation from medical procedures such as diagnostic X-rays, comprise approximately 35% of an average Australian citizen's total annual exposure (Figure 1-1).

The current model for radiation risk assessment, termed the linear no-threshold model (LNT), states that all doses of radiation including extremely low doses, are harmful. This model suggests a proportional relationship between dose and cancer risk (as reviewed by Tubiana et al., 2006; 2009). It is becoming increasingly apparent that the LNT model could lead to incorrect assumptions of safe radiation exposure. This model is based predominantly on epidemiological data obtained from Japanese atomic bomb survivors, and a linear extrapolation is used for doses below 100 mSv (Figure 1-2) and is extrapolated for doses below 100 mSv. Furthermore, the disparity between the biological effects of low and high dose radiation exposure indicate that little is still known regarding the mechanism(s) involved in the response(s) to radiation damage, and the doses that can potentially lead to radiation-induced cancer.

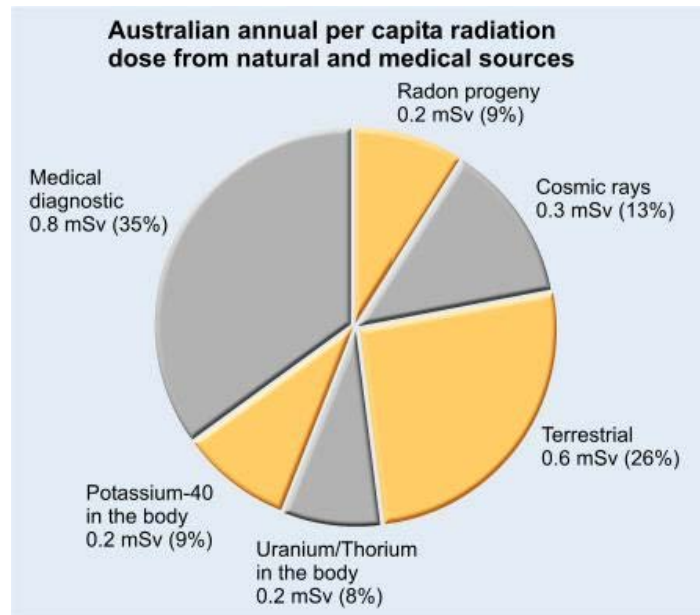


Figure 1-1: Sources of radiation exposure.

Natural and medical sources of radiation exposure (mSv) in Australia per capita.

Obtained from: <http://www.arpansa.gov.au/radiationprotection>. Accessed: 10th July, 2012.

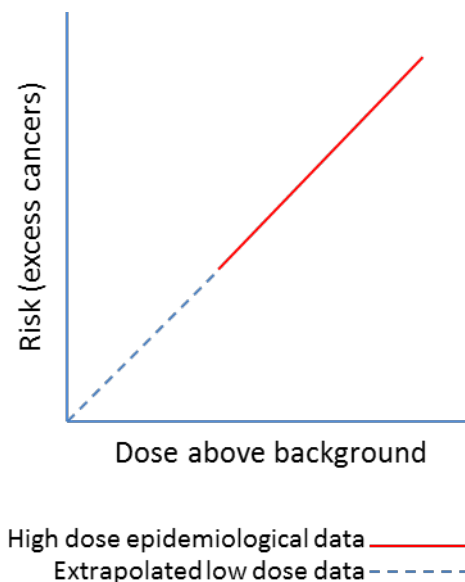


Figure 1-2: Linear no-threshold model.

The linear no threshold model is based on epidemiological data (solid red line), which is extrapolated for doses less than 100 mSv (broken blue line) and predicts that all doses of radiation above background exposure increase cancer risk proportionally.

1.1 Ionising Radiation

Radiation can be categorised as ionising or non-ionising. The classification of radiation type is based on the amount of energy available for transfer to biological material. Non-ionising radiation does not have enough energy to directly break chemical bonds. Examples of non-ionising radiation include microwaves and visible light. Ionising radiation can be categorised as radiation waves (X- and gamma (γ)-rays) or radiation particles such as α - and β -particles. X-rays are a man-made form of ionising radiation and are produced by energy transitions due to accelerating electrons. The α - and β -particles and γ -rays are naturally occurring forms of ionising radiation and are emitted from the decay of naturally occurring isotopes. Gamma-rays can also be produced from atmospheric interactions with cosmic rays. Ionising radiation is biologically hazardous due to its high energy which enables it to disrupt chemical bonds (as reviewed by the U.S. Environmental Protection Agency, 2007a; 2007b; Raabe, 2012). Radiation effects can be classified as “deterministic” or “stochastic”. The tissue effects of ionising radiation exposure are termed “deterministic effects”, that is, the direct effects of the ionising radiation exposure such as organ failure, which occurs when the number of cells undergoing apoptosis outweighs the ability of the cell to replace them (Edwards and Lloyd, 1998). “Stochastic effects” of ionising radiation exposure are defined as the damage that can occur at the DNA level resulting in genomic instability and cancer at a later time-point (sometimes years) following the irradiation (Edwards and Lloyd, 1998).

1.1.1 Quantifying ionising radiation

The different types of ionising radiation are classified based on their linear energy transfer (LET). X-rays are low LET, and can penetrate deep into tissues. However, they are sparsely ionising and deposit energy randomly. Alpha particles are considered to be high LET and have the ability to ionise atoms, and are therefore highly destructive to a cell. Radiation is measured based on activity and exposure. The activity is measured as a standard international unit (SI) called the Becquerel (Bq) which is a unit of radioactive decay equal to one disintegration per second. Exposure to ionising radiation is measured as absorbed dose, equivalent dose and effective dose (Figure 1-3).

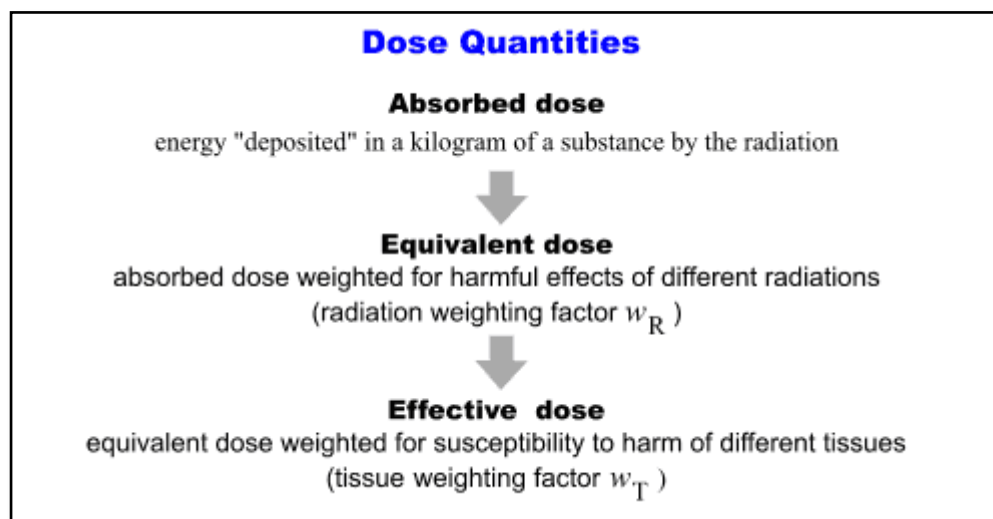


Figure 1-3: Measurement of radiation exposure.

Description of the measurement of radiation exposure of energy deposited in relation to the type of radiation i.e. α - particles or X-rays and the effect of the absorbed dose on tissues.

Adapted from: <http://www.arpansa.gov.au/radiationprotection/basics/units.cfm>. Accessed: 11th July, 2012.

Absorbed dose is measured in an SI unit of Gray (Gy). A Gray is the amount of absorbed energy deposited in one kilogram of mass. Not all types of radiation have the same biological effect for the same amount of absorbed dose, and therefore a measurement known as the equivalent dose, a Sievert (Sv) is used. The equivalent dose is determined by the absorbed dose multiplied by the weighting factor (W_R) of the radiation type. The weighting factor takes into account that some types of radiation produce more biological damage compared with others of the same absorbed dose. For example, X-rays have a W_R of 1, whilst α -particles have a W_R of 20; and hence 1 Gy X-rays equals 1 Sv, while 1 Gy α -particles equals 20 Sv. Finally, the effect on different tissues and organs that radiation will have is taken into account when quantifying radiation. This incorporates a tissue weighting factor (W_T ; Figure 1-4) to calculate the effective dose (E) to an organ (Sv), which is the equivalent dose of a radiation type multiplied by the tissue weighting factor. For example, tissue weighting factors will be used to determine the effective doses that different types of medical X-rays will have depending on the susceptibility to radiation-induced damage of the tissues and organs that are being imaged.

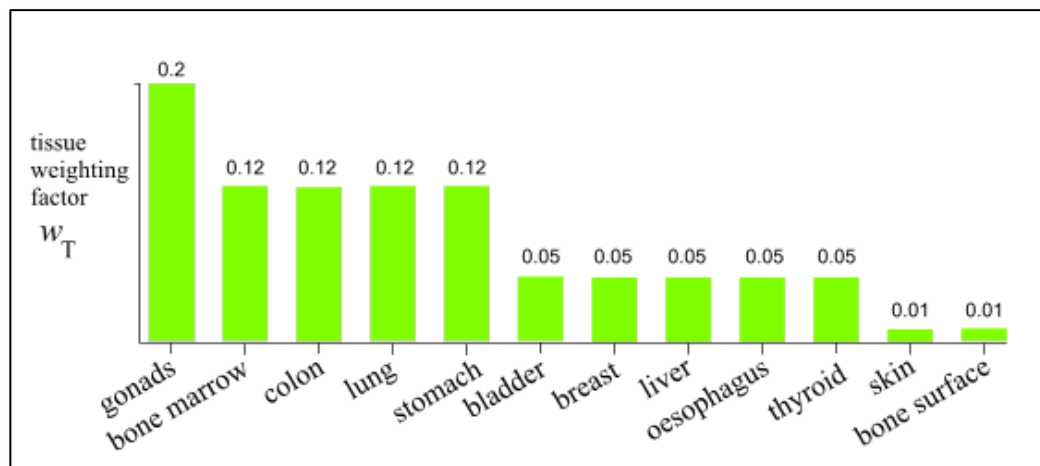


Figure 1-4: Tissue/organ radiation weighting factors.

The weighting factor for human tissues/organs for determining effective doses following radiation exposure.

Adapted from: <http://www.arpansa.gov.au/radiationprotection/basics/units.cfm>. Accessed: 12th July, 2012.

1.2 Biological Effects of Radiation

1.2.1 Mouse models in radiation research

The use of mice in research has become a powerful tool in the elucidation of the mechanisms that drive diseases such as cancer and diabetes, heart disease, as well as the effects of exogenous factors such as exposure to chemical carcinogens, diet and radiation. Mouse models provide insight into physiological and homeostatic responses that cannot be replicated *in vitro*. In radiation research, the mouse model is a particularly useful tool for understanding the effects of radiation on the whole organism, at the tissue, cellular and DNA level as well as specific systems such as the immune system. The most commonly used mouse strains in radiation research include the *scid* (severe compromised immunodeficiency), C57Bl/6, BALB/c and CBA

mouse strains. Grahn and Hamilton (1957), and Roderick (1963) investigated the effect of radiation exposure on inbred mouse strains, determining that some were more sensitive to radiation than others. Both studies demonstrated that the BALB/c followed by the CBA mouse strain were the most radiosensitive strains, while the C57Bl/6 strain exhibited less sensitivity to the radiation exposure. *Scid* mice are also extremely sensitive to radiation exposure due to a lack B and T-cells and deficiencies in DNA repair pathways. This strain is a good model organism for investigating the role of the immune system in response to ionising radiation (Fulop and Phillips, 1990; Biedermann *et al.*, 1991). BALB/c mice also exhibit deficiencies in DNA repair, and develop radiation-induced mammary cancers, leukaemia and other solid tumours (Storer *et al.*, 1988; Okayasu *et al.*, 2000). The CBA mouse strain is most commonly used in the study of leukaemogenesis, demonstrating low spontaneous leukemic frequency, but upon radiation exposure will develop acute myeloid leukaemia (AML) similar to human AML subsets (Rithidech *et al.*, 1999). While described as radiation resistant, C57Bl/6 mice can develop radiation-induced thymic lymphoma, which is most efficiently induced by repeated exposure to whole body irradiation with 1.8 Gy (Kaplan and Brown, 1952; Ina *et al.*, 2005), but on the whole can survive doses of radiation which would induce mortalities in the aforementioned strains (see Table 1 and Table 2). As a result, numerous studies have utilised these mice for the investigation of DNA repair pathways (Biedermann *et al.*, 1991; Okayasu *et al.*, 2000; Yu *et al.*, 2001), the induction of radiation-induced leukaemia (Plumb, 1998; Boulton, 2001; 2003; Giotopoulos *et al.*, 2006), haematopoietic recovery (Yugas and Storer, 1969; Hamasaki *et al.*, 2007) and differences in p53-mediated apoptosis in response to radiation exposure (Lindsay *et*

al., 2007). It should be noted that the three mouse strains discussed, C57Bl/6, BALB/c and CBA, all exhibit functional p53 responses, although the BALB/c strain has been reported to display reduced transcriptional activity in comparison to the C57Bl/6 mouse strain (Feng *et al.*, 2007; Lindsay *et al.*, 2007). Engineered mouse strains that contain mutations are also used, such as the Trp53 homozygous mice. These mice contain a mutated allele of the p53 gene and are used to understand the role that p53 plays in both radiation-induced carcinogenesis and the low-dose radioadaptive response (Mitchel *et al.*, 2003; 2004; 2008). Mouse studies are also a powerful tool for investigating the transgenerational effects of radiation exposure.

Table 1: LD_{50:30} of inbred mouse strains following single whole body X-irradiation.

Strain	Male		Female	
	LD _{50:30} ^a	SE	LD _{50:30} ^a	SE
BALB/cJ	<5.7		5.85	0.12
A/J	5.9	0.2	6.42	0.08
RF/J	6.28	0.2	7.13	0.15
SWR/J	6.29	0.1	6.14	0.06
C57BL/6J	6.5	0.15	6.7	0.06
CBA/J	6.56	0.09	6.89	0.08
C3HeB/J	6.76	0.11	6.89	0.07
SJL/J	7.13	0.11	7.74	0.13
C57BR/J	7.29	0.09	7.38	0.08
129/J	7.34	0.1	7.74	0.13

^adose of X-irradiation not specified

Adapted from the Biology of the Laboratory Mouse (Green, 1966)

Table 2: Days survival following daily whole-body X-irradiation with 10 Gy of the C57Bl/6, BALB/c and CBA mouse strains in a study of twenty-seven mouse strains.

Strain	<i>Male</i>		<i>Female</i>		Ranking in comparison to other strains ^b
	No. Days	SE	No. Days	SE	
C57Bl/6	24.58	1.18	23.03	0.42	14/27
BALB/c	17.00	0.45	16.76	0.48	26/27
CBA	16.44	0.56	16.55	0.55	27/27

^bAdapted from Roderick (1963)

1.2.2 High dose radiation exposure

1.2.2.1 Tissue effects from high dose radiation exposure

The effects of high dose radiation (HDR) exposure are most apparent in tissues such as bone marrow, thymus, spleen, gastrointestinal tract and lymphatic tissue – tissues that display high cellular turnover. HDR changes the tissue microenvironment, which can affect cell phenotype, tissue structure and signal transduction. This can result in persistent inflammation, which leads to greater cellular, and ultimately, tissue destruction (reviewed by Liu, 2010). High enough doses of radiation (>10 Sv) cause acute radiation sickness and symptoms such as gastrointestinal disorders can be evident within hours, while other symptoms can include bacterial infections, haemorrhaging, anaemia, loss of body fluids and electrolytes (as discussed by the U.S. Environmental Protection Agency, 2007b). Widespread cell death, or impaired activity within an organ or a tissue will result in the loss of organ function (as discussed by the Recommendations of the International Commission on Radiological Protection 2007).

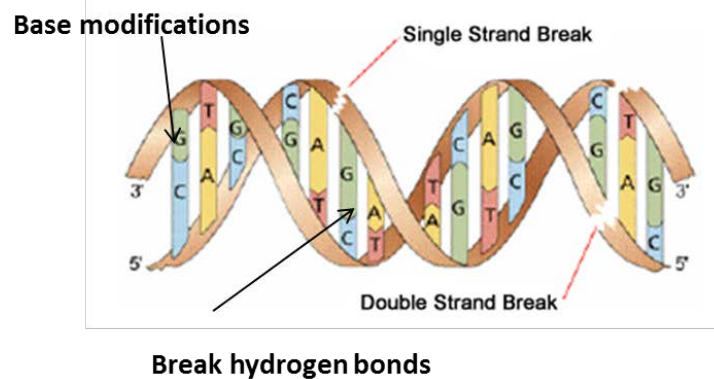
1.2.2.2 Sub-cellular effects from high dose radiation exposure

At the DNA level, there are three main outcomes of radiation exposure: 1) DNA lesions will result in the cell attempting to repair the damage induced. If the repair has been error free and the DNA is restored to its normal state, there will be no consequence to cell fate and therefore no risk of cancer; 2) the cell cannot repair the resulting DNA damage and programmed cell death (apoptosis) is induced. The damaged cell is removed and there is no risk of cancer. 3) The cell repairs the DNA damage, but with errors. The cell may detect the incorrectly repaired DNA and still activate apoptosis, or it may fail to detect the DNA damage thus allowing the cell to remain. DNA aberrations and mutations following the initial irradiation can lead to genomic instability, which is characterised by an increased rate of mutation. While mutations drive genetic diversity and therefore may not always result in a deleterious phenotype, genomic instability can lead to cancer.

Ionising radiation induced damage primarily affects DNA. This can be via direct or indirect ionisation of the DNA strands. Direct damage occurs from the electron track through the cell, causing proton loss of the sugar-phosphate backbone, resulting in single strand breaks (SSBs), and less frequently, double strand breaks (DSBs) of the DNA. Oxidation of the bases can lead to modified bases such as 8-hydroxyadenine and thymine dimers. Indirect damage to DNA following ionising radiation is the generation of reactive oxygen species (ROS) by the hydrolysis of water producing singlet oxygen atoms, hydroxyl radicals, superoxide radicals and hydrogen peroxide. The hydroxyl radicals (OH•) are considered to be the most damaging ROS, and can also be produced by the reduction of hydrogen peroxide. The hydroxyl radicals cause damage to the sugar-phosphate backbone, bases and results in SSB and DSBs

also (Figure 1-5). Most damage arising from ROS occurs from the indirect, hydroxyl radical damage (65% of the induced damage), compared to the damage induced by direct ionisation (35%) (Table 3)(Ward, 1988; Goodhead, 1989; Ward, 1990; Goodhead, 1994; Riley, 1994; Ward, 1995; Goodhead, 2009). Complex, clustered lesions in DNA (damages within one helical turn of each other) or DNA double strand breaks (DSB) are considered to be the most lethal type of DNA damage following ionising radiation exposure. Radiation-induced cell death can be due to errors in, or a lack of DNA repair at sites of damage. Persistent transgenerational changes to DNA can occur as a result of mutations arising from excessive damage or errors in repair (Charlton *et al.*, 1989; Goodhead, 1994; Barber *et al.*, 2002; 2006; Goodhead, 2009; Wright, 2010).

Direct damage



Break hydrogen bonds

Indirect damage

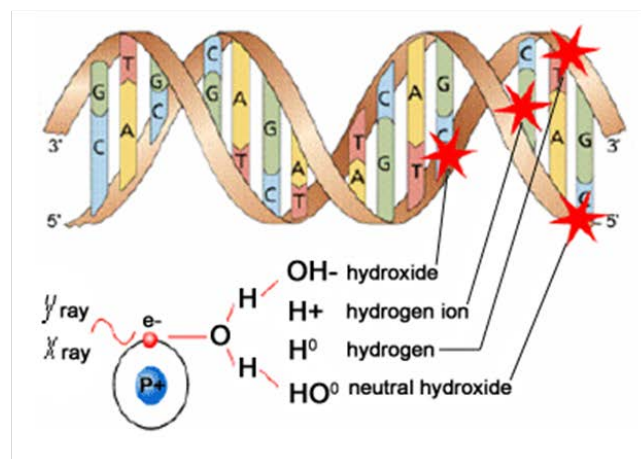


Figure 1-5: Damage to DNA following high dose radiation exposure.

DNA damage can occur following ionising radiation exposure either directly or indirectly. Direct damage occurs when the electron track occurs through the DNA causing proton loss to the sugar backbone, causing single strand and double strand breaks, inducing base damage or breaking the hydrogen bonds between bases. Indirect damage is the result of ionisation of water molecules, producing reactive oxygen species, of which the most damaging is the hydroxyl radical. These also cause damage to the sugar backbone, modify bases and break hydrogen bonds. Adapted from: <http://www.cna.ca/curriculum>. Accessed on the 19th September, 2012.

Table 3: Number of events of the different types of DNA damage that can occur in a cell following irradiation with 1 Gy X-rays.

	Damage	Number of events
Initial physical damage	ionisations in cell nucleus	100 000
	ionisation directly in DNA	2000
Biochemical damage	SSBs	1000
	8-hydroxyadenine	700
	thymine damage	250
	DSBs	40
	DNA-protein cross links	150

Adapted from Goodhead (1994)

1.2.2.3 Repair of DNA following high dose radiation exposure

DSBs damage both DNA strands and prevent the use of the complementary DNA strand as a template for repair, while for SSBs, the complementary strand can be used as a template for the new strand. Repair of DNA strand breaks is via base excision repair (BER), nucleotide excision repair (NER), mismatched repair (MMR), non-homologous end joining (NHEJ), or homologous recombination (HR). BER repairs non-helix distorting base modifications, abasic sites and SSB. It recognises and removes the inappropriate bases, while enzymes create an abasic site intermediate that is cleaved and the gap is filled in. NER can be involved in global repair or transcription-coupled repair, at places where RNA polymerase elongation has been blocked, removing thymidine dimers and bulky DNA adducts. MMR removes small mismatches, insertions and deletions that arise during replication or recombination. HR uses undamaged sister chromatid templates to repair DNA. DSBs caused by recombination are repaired by NHEJ machinery (reviewed by van Gent *et al.*, 2001; Kulkarni and Wilson, 2008). DSBs can also be caused by replication and

V(D)J gene recombination (the process by which immunoglobulin genes are rearranged to create immune diversity). Deficiencies in DNA repair mechanisms, such as in *scid* mice, have shown an inability to repair the damage induced by both V(D)J recombination and radiation (Biedermann *et al.*, 1991). Inefficient DNA repair as a result of ageing can result in the same accumulation of DSBs as induced by radiation exposure. Sedelnikova *et al* (2004) found that there was an accumulation of DSBs in ageing mice and also in cell cultures that had been allowed to reach senescence. The accumulation of DSBs in the cultured cells was equivalent to those induced in cells exposed to HDR. This indicates that regardless of the source of DNA damage, excessive damage still affects a cell's ability to repair the damage.

1.2.3 Low dose radiation exposure

According to the LNT model, all doses of radiation above background exposure no matter how small can increase cancer risk. However, there is increasing evidence indicating that low dose radiation (LDR) exposure does not elicit the same effect as high dose radiation exposure (HDR), and in some studies has been shown to be able to reduce the effect that HDR has on a cell/organism (as discussed by Dauer *et al.*, 2010). This has been termed the low dose radioadaptive response, and has been observed in a diverse range of organisms including bacteria, plants, yeast and animals (as discussed by Sakai *et al.*, 2006). A radioadaptive response is defined as "A post-irradiation cellular response which, typically, serves to increase the resistance of the cell to a subsequent radiation exposure" (Valentin, 2007).

The first radioadaptive response experiment reported showed that human lymphocytes cultured in ^3H thymidine had less chromosomal aberrations following exposure to X-radiation than cells exposed to the ^3H thymidine or X-rays alone (Olivieri *et al.*, 1984). Since then, many studies have demonstrated that a low dose of radiation can protect from the DNA damage induced by HDR exposure for a number of end-points including DNA DSB formation (Stoilov *et al.*, 2007) and micronuclei (Venkat *et al.*, 2001; Broome *et al.*, 2002; Mitchel, 2006). In animal studies, low doses have also been shown to reduce intra-chromosomal recombination in transgenic mice to below endogenous frequencies, as well as reduce the damage induced by a HDR exposure (Hooker *et al.*, 2004; Day *et al.*, 2006a; 2006b; Zeng *et al.*, 2006; Day *et al.*, 2007a), even if the high dose is delivered prior to the low dose (Day *et al.*, 2007b). In one study, it was demonstrated that the protection induced by the LDR still induced protection from a HDR exposure given 1 year after the LDR exposure, and was also able to reduce the accumulation of endogenous mutations over the life of an ageing animal (Zaichkina *et al.*, 2006). The radioadaptive response has also been demonstrated to be cross-adaptive, where one agent (such as LDR) can induce an adaptive response for a different agent. For example, conditioning doses of X-rays were demonstrated to be able to reduce mutations induced by treatment with an alkylating agent in mice (Yamauchi *et al.*, 2008).

While HDR exposure increases DNA damage and the frequency of mutations, which can ultimately lead to cancer, LDR has been reported to reduce cancer incidence. Single or multiple exposure to LDR (50 -100 mGy) has been demonstrated to reduce the incidence of thymic lymphoma, spontaneous and HDR-induced tumour

formation, as well as delay tumour formation in mice (Ishii *et al.*, 1996; Mitchel *et al.*, 2003; 2004; Ina *et al.*, 2005; 2007; 2008). LDR has also been shown to selectively inhibit damage to non-tumour cells when exposed to HDR in comparison to tumour cells (Jiang *et al.*, 2008); as well as induce the selective removal of pre-cancerous lesions (Portess *et al.*, 2007) and reduce neoplastic transformation frequency (Azzam *et al.*, 1994; 1996; Redpath *et al.*, 2001; Elmore *et al.*, 2008).

There is increasing evidence that the radioadaptive response may involve stimulation of the immune system, promoting increased efficiency to remove both damaged and cancerous cells. Exposure to LDR has been shown to increase the number of tumour tissue-infiltrating lymphocytes (Hashimoto *et al.*, 1999) and stimulate natural killer cell mediated cytotoxic activity (Cheda *et al.*, 2004). In addition to increased cytotoxic activity, there have also been reports of increased proliferation and repopulation of bone marrow/haematopoietic cells following LDR exposure (Matsubara *et al.*, 2000; Wang and Cai, 2000; Li *et al.*, 2004; Ina *et al.*, 2005).

1.2.4 Ageing and radiation exposure

Ageing is associated with an increased accumulation of DNA damage and an increased risk of cancer (as reviewed in Gorbunova *et al.*, 2007; Calvanese *et al.*, 2009). Age has been shown to influence radiation sensitivity (Lindop and Rotblat, 1962; Vesselinovitch *et al.*, 1971; Sasaki, 1991; Kato *et al.*, 2011), while reduced effectiveness of the adaptive response in *ex vivo* cells from elderly individuals has been observed (Gadhia, 1998). *In vitro* experiments in rodent cells have

demonstrated that glial cells from aged rats did not show an adaptive response compared with the cells from young rats (Miura *et al.*, 2002). In contrast, *in vivo* animal studies have shown that age at irradiation does not influence the radioadaptive response (Zaichkina *et al.*, 2006). The disparity between these experiments may be due to the endpoints analysed, tissues investigated, animal models used, dose and dose-rate, and highlights that further investigation on the relationship between the radioadaptive response and ageing is needed.

1.3 Maintenance of genomic stability

Both ageing and the effect of HDR exposure are characterised by reduced genomic stability. Genome stability (correct gene expression, protein functions and correct repair of DNA) is maintained by numerous mechanisms including histone modifications, telomere caps and DNA methylation. These modifications of DNA are stably inherited and work synergistically to influence the structure of chromatin, thereby controlling gene expression.

1.3.1 Chromatin structure

DNA methylation (discussed in Section 1.3.2) along with histone modification marks have been shown to be involved in the regulation of chromatin structure and promoter availability to transcriptional machinery, and ultimately gene expression.

Chromatin consists of DNA/protein structures called nucleosomes. The nucleosome consists of an octamer of four histones – H3, H4, H2A and H2B. Wrapped around

this octamer is ~147 bp of DNA. The histone proteins have N-terminal tails which can undergo post-translational modifications (marks) that include acetylation, methylation, phosphorylation, ubiquitination, sumoylation, ADP-ribosylation, deimination and proline isomerization. These histone marks influence the compaction and structure of the chromatin. For example, acetylation of histone H3 is associated with transcription and DNA repair, as it promotes an “open” chromatin structure, while lysine methylation is associated with repression of gene expression as it promotes a “closed” chromatin structure (Figure 1-6). CpG methylation also influences chromatin structure by inducing overwrapping of the DNA around the histone octamer (reviewed by Lee and Lee, 2011), and acting as a recruiting point for methyl binding proteins which form a platform. This platform recruits histone deacetylases (HDAC) that remove acetyl groups from the N-terminal tails, which in turn recruits histone lysine methyltransferases. It has been reported that these histone modifications then recruit proteins which bind the *de novo* DNA methyltransferases, which become anchored to the nucleosome, enhancing the repression (Sharma *et al.*, 2011). Therefore, heterochromatin regions are associated with reduced acetylation, increased histone H3 lysine 9 residue methylation and CpG methylation, while euchromatic regions are associated with increased acetylation, and reduced lysine and CpG methylation, and exhibit active transcription.

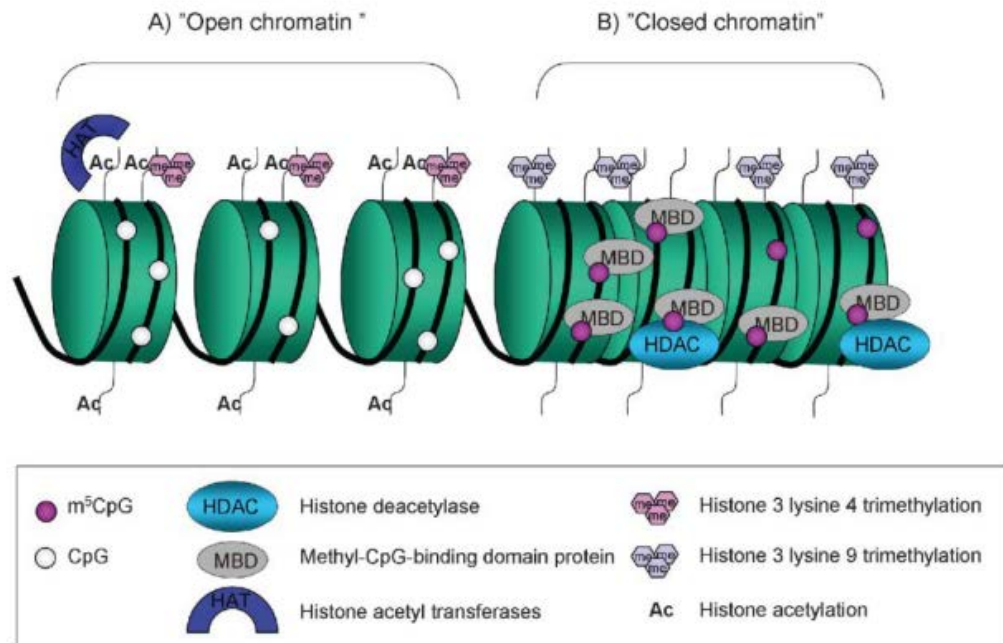


Figure 1-6: Control of chromatin structure by epigenetic modifications.

(A) Transcriptionally active chromatin is characterised by unmethylated cytosines (CpG) and acetylated histone tails. (B) Methylated cytosine residues ($m^5\text{CpG}$) bind methyl binding domain proteins (MBD) that attract histone deacetylases (HDAC), which then remove acetyl (Ac) groups from the histone tails. The DNA becomes coiled into a "closed" chromatin structure carrying the silencing mark histone H3 lysine 9 tri-methylation. Adapted from Gronbaek et al (2007).

It has been shown that chromatin structure influences and is influenced by DNA repair mechanisms. It has been suggested that DNA damage in heterochromatin elicits faster repair responses compared to euchromatin due to the topology of the heterochromatin and the requirement to suppress any reactivation of transposable elements (Jakob *et al.*, 2011). However, other studies have shown that due to the tightly compacted nature of heterochromatin, it is repaired later than euchromatin (Cowell *et al.*, 2007; Goodarzi *et al.*, 2008; Chiolo *et al.*, 2011). Regardless, it is evident that following DSB formation, the DNA repair protein ATM phosphorylates the histone H2A variant, H2AX (termed γH2AX). This then provides a docking

platform for other repair proteins, and also involves “eviction” of the nucleosome from the damaged DNA region, unwinding the DNA (Xu and Price, 2011). In order to unwind the DNA, CpG demethylation occurs. At the time γ H2AX is recruited to the site of the DSB, the DNA methyltransferase DNMT1 is also recruited, interacting with ATM (Mortusewicz *et al.*, 2005; Ha *et al.*, 2011), and other repair proteins such as GADD45 α (Barreto *et al.*, 2007; Lee *et al.*, 2011). The DNA methylating activity of DNMT1 is inhibited during this process, and leads to active demethylation of CpGs (Barreto *et al.*, 2007; Lee *et al.*, 2011). Thymine DNA glycosylase (TDG) is also implicated in DNA demethylation associated with base-excision repair, which results in destabilisation of the chromatin. The *de novo* methyltransferases are recruited during this process and are involved in the regulation of TDG and the subsequent re-methylation of the DNA (Li *et al.*, 2007). Following DNA repair, besides the restoration of CpG methylation, chromatin re-assembly and restoration of the nucleosome requires acetylation of histone H3 (Chen *et al.*, 2008).

Aberrant chromatin structure is associated with cancer, and is generally in the form of compacted chromatin, exhibiting increased lysine and CpG methylation and reduced acetylation (Nguyen *et al.*, 2002; Tryndyak *et al.*, 2006; Kondo *et al.*, 2007). These aberrations result in the incorrect gene expression patterns observed at proto-oncogenes and tumour suppressor genes. However, heterochromatic regions begin to exhibit properties of active euchromatin in the form of increased acetylation and reduced lysine and CpG methylation, which can result in transposition of repeat elements and microsatellite expansion (Fraga *et al.*, 2005; Howard *et al.*, 2007; Daskalos *et al.*, 2009; Estecio *et al.*, 2010; Muotri *et al.*, 2010; Ryu *et al.*, 2011).

1.3.2 DNA methylation

DNA methylation is a chemical modification to the fifth position of the cytosine pyrimidine ring. 5-methylcytosine (5mC) is generated when a methyl group from the universal methyl donor S-adenosylmethionine (SAM) is added via the DNA methyltransferase enzymes (DNMTs), which catalyse the transfer (Figure 1-7). A methylated cytosine in the context of DNA will be hitherto known as 5-methyldeoxycytidine (5mdC). Methylation of cytosine occurs during DNA replication, whereby the methylation pattern on the parental DNA strand is copied onto the newly synthesised strand by the maintenance methyltransferase DNMT1. *De novo* methylation, the process whereby a methyl group is added to a cytosine residue when there is no parental template, is performed by the methyltransferases DNMT3a and DNMT3b. These DNMTs play a large role in establishing methylation patterns during development (Costello and Plass, 2001; Curradi *et al.*, 2002; Liang *et al.*, 2002; Gronbaek *et al.*, 2007; DeAngelis *et al.*, 2008). In mammalian genomes, approximately 2-10% of cytosines are methylated. DNA methylation mainly occurs at a cytosine residue that is next to a guanine in sequence, separated by a phosphate that links the nucleotides. This is termed a CpG dinucleotide. Approximately 70-80% of the CpGs within the genome are methylated, however the majority of CpGs located within gene promoters are unmethylated. CpG-rich regions, known as CpG islands are most heavily methylated within heterochromatin, regions that contain repeated DNA elements. Heavy DNA methylation is also found to be involved in imprinting and X-inactivation, and patterns of methylation are tissue and development specific (Lorenz *et al.*, 1955; Puntschart and Vogt, 1998). During embryogenesis, the genome undergoes a wave of controlled demethylation,

following which *de novo* methylation occurs to establish methylation patterns that will be maintained.

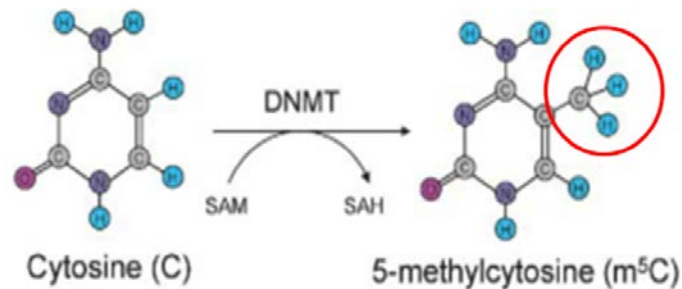


Figure 1-7: Methylation of cytosine.

Cytosine residues in DNA are converted to 5-methylcytosine by DNA methyltransferases (DNMTs). The universal methyl donor S-adenosylmethionine (SAM), which is converted to S-adenosylhomocysteine (SAH), donates the methyl group (ringed in red). Adapted from Gronbaek et al (2007).

DNA methylation levels can be altered by ageing (Wilson *et al.*, 1987; Christensen *et al.*, 2009) or exogenous factors such as diet (e.g. folate, which is a methyl donor), exposure to chemicals found in pollution (Yauk *et al.*, 2008), cigarette-smoke (Damiani *et al.*, 2008; Christensen *et al.*, 2009) and asbestos (Christensen *et al.*, 2009). In response to these modulators, a loss of DNA methylation is commonly observed and can result in increased mutation rates (Yauk *et al.*, 2008), increased frequency of cellular transformation and micronuclei formation (small nuclei formed as a result of damage to chromosomes) (Damiani *et al.*, 2008).

Research has demonstrated that there is a link between DNA damage and altered CpG methylation. Valinluck *et al* (2007) reported that inflammation-induced DNA-damaging products such as 5-chlorocytosine, mimic 5mdC and induce inappropriate

DNMT1 methylation within a CpG sequence. DNA methylation damage can also occur due to the conversion of 5mdC to thymine glycol by endogenous ROS, or an exogenous ROS-inducing agent such as ionising radiation. Oxidation of 5mdC can result in mismatches within the DNA sequence and can contribute to the increased number of transition mutations observed at methylated cytosine residues (Figure 1-8). Deamination of 5mdC can be followed by T:G base-excision repair by glycosylases, which can lead to an inherited loss of methylation at that CpG site (Slupphaug *et al.*, 2003; Popp *et al.*, 2010). An association between DNA DSBs and reduced or aberrant DNA methylation has been demonstrated, where a loss of methylation can result in excess DSB formation following exposure to DNA damaging agents (Beetstra *et al.*, 2005; Palii *et al.*, 2008). Furthermore, DNMT1 has been found to co-localise with γ -H2AX at sites of DSBs (Mortusewicz *et al.*, 2005; Palii *et al.*, 2008; Ha *et al.*, 2011), and aberrant DNMT1 protein levels have also been linked with aberrant *de novo* methylation of tumour suppressor genes, and reduced DNA repair (Trasler *et al.*, 2003; Ray *et al.*, 2006; Kondo *et al.*, 2007; Damiani *et al.*, 2008).

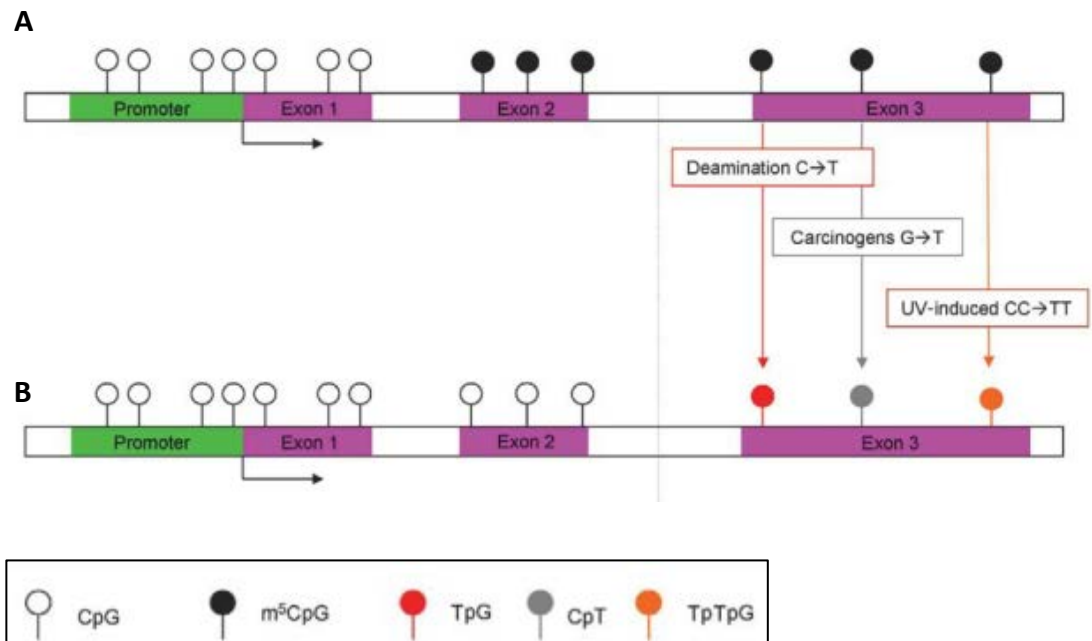


Figure 1-8: Facilitation of mutations via demethylation of cytosine.

(A) Methylated cytosine within the coding regions of genes may facilitate mutations by spontaneous hydrolytic deamination to thymine ($5mC \rightarrow T$), by exposure to carcinogens (resulting in $CpG \rightarrow CpT$ mutations), or UV-induced thymine adducts (resulting in $CCpG \rightarrow TTpG$). (B) Abberant methylation of promoters following repair. Adapted from Gronbaek et al (2007).

1.3.2.1 Methods for the detection of DNA methylation

There are a number of methods that are utilised to analyse CpG methylation. The choice of technique used is influenced by the experiment being performed, e.g. determination of the methylation levels at single gene loci vs. total genomic 5mdC.

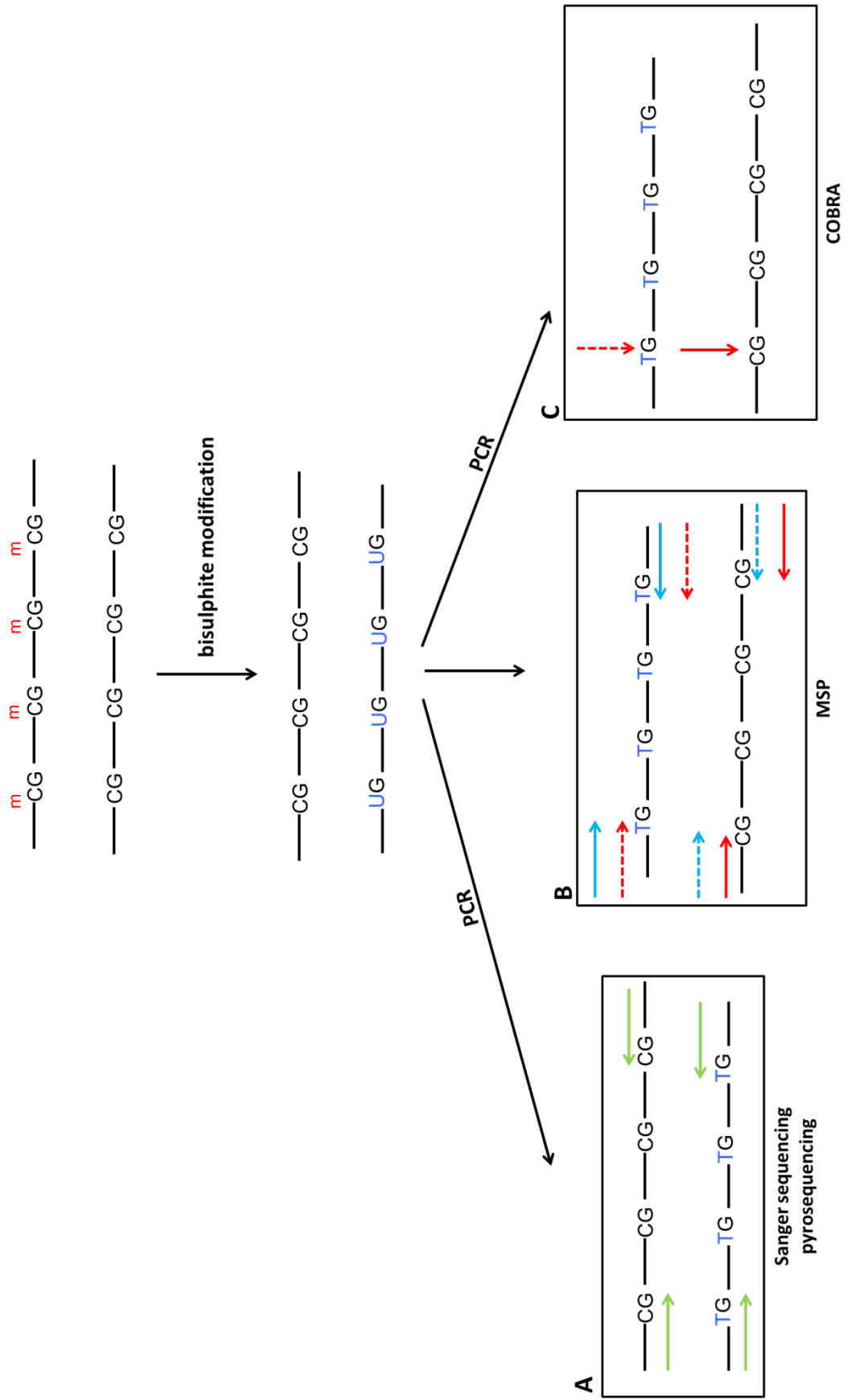
1.3.2.1.1 Single gene loci

Sodium bisulphite is most often used in the investigation of the methylation status of CpGs located within the promoters of gene loci. Sodium bisulphite treatment allows the distinction between cytosine residues that have a methyl group and

cytosine residues that are unmethylated. Following treatment of DNA with sodium bisulphite, unmethylated cytosines are converted to a uracil whereas a methyl group will protect the cytosine from conversion (Frommer *et al.*, 1992; Chen and Shaw, 1993). This process creates distinct sequences of DNA based on methylation status. PCR is then predominantly used to assess the methylation status of the target region (CpGs of interest) (Figure 1-9). The PCR products can be analysed using Sanger sequencing or pyrosequencing, methylation-specific PCR (MSP) or combined bisulphite restriction analysis (COBRA). Pyrosequencing detects pyrophosphate release upon nucleotide incorporation, allowing the level of fluorescence to be quantified at an individual CpG site. For MSP, separate primers specific for methylated versus unmethylated DNA are used. The methylation status of the CpG is then determined based on successful amplification with one of the primer sets. COBRA utilises methylation-sensitive restriction enzymes to determine methylation status. Restriction enzymes such as *HpaII* are chosen based on their sensitivity to methylated CpGs within the recognition sequence of the enzyme. An enzyme that would normally be unable to digest unmodified DNA due to the presence of a methyl group is able to cut DNA following bisulphite modification and PCR. DNA that was unmethylated prior to bisulphite modification will have a thymine in the recognition sequence following bisulphite modification and PCR, and will not be digested. Therefore, the methylation status of a CpG within the PCR product can be described as being methylated if the PCR product is digested, and unmethylated if undigested.

Figure 1-9: Techniques that utilise bisulphite modification to evaluate methylation levels.

When genomic DNA (gDNA) is treated with sodium bisulphite, cytosine residues that do not contain a methyl group will be converted to a uracil, while methylated cytosines will remain as a cytosine. The methylation status of a single gene locus can be determined following PCR (during which uracil residues are replaced by a thymine residue) by (A) Sanger sequencing or pyrosequencing of the PCR products (green arrows indicate sequencing primers); or (B) designing PCR primers that are specific for methylated CpGs (red arrow) or unmethylated CpGs (blue arrows). If the unmethylated-specific primers successfully amplify, the target region is unmethylated, and vice versa. This is known as Methylation-Specific PCR (MSP). (C) Following PCR, methylation sensitive enzymes can be used to digest the PCR products. Enzymes that would normally be unable to digest DNA if a methylated cytosine is within the recognition sequence will be able to digest DNA following bisulphite modification (red arrow), while unmethylated cytosine residues are converted to a uracil and the the enzyme no longer recognises the site (broken red arrow)(COBRA – combined bisulphite restriction analysis).



Although commonly used in methylation studies as these techniques are rapid and inexpensive, there are limitations. Pyrosequencing is limited to approximately 30 nucleotides, and is inhibited by the presence of non-CpG single nucleotide polymorphisms (SNPs). MSP is limited to only one CpG, while COBRA depends on efficient enzyme activity. Furthermore, in a target region that contains more than one CpG, heterogeneous methylation needs to be considered. Sanger sequencing can provide detailed information about the methylation status of individual CpGs when PCR products are cloned and single amplicons are sequenced, however this is laborious and low throughput. A post-PCR technique known as high resolution melt analysis (HRM) is also utilised to determine the methylation status of a target region that contains more than one CpG. Following quantitative real-time PCR, PCR products are subjected to increasing temperatures until the DNA strands become single stranded (ssDNA). Upon becoming single stranded, a fluorophore which was bound to the double stranded PCR products (dsDNA), is released. The temperature range at which fluorescence is detected is recorded. DNA that is GC rich requires greater temperature to break bonds and create ssDNA compared with DNA that is AT rich. Therefore, following bisulphite modification, DNA that is methylated will have a greater GC composition than unmethylated DNA, where all unmethylated cytosines were converted to a uracil. Thus, heterogeneously methylated DNA can be distinguished from fully methylated and unmethylated DNA, based on melting properties.

1.3.2.1.2 Genome-wide methylation

A reduction in total genomic 5mdC levels is a hallmark of cancer, along with the hypermethylation of certain loci. Hence, genome-wide methods for analysing DNA methylation are commonly performed in methylation studies. High purity liquid chromatography (HPLC) was first utilised to assess total genomic DNA methylation levels. Since then the more sensitive liquid chromatography-mass spectrometry (LC-MS) has been used. While highly sensitive, these techniques are not able to give the location of the CpGs that have been modulated, and are not ideal for analysing a large number of samples. This has led to next generation sequencing platforms being used to investigate genome-wide DNA methylation changes, to determine where these changes are occurring. While high-throughput, these platforms can be expensive and not available to all laboratories, and require complicated bioinformatics to process the data.

The methylation-sensitive enzyme *HpaII* and its isoschizomer *MspI* are also used in genome-wide methylation studies. The proportion of DNA that is digested by *HpaII* relative to *MspI* is used to determine the methylation levels of samples. An adaptation of this technique is the cytosine extension assay (Pogribny *et al.*, 1999). Following digestion of the DNA, radiolabelled cytosine is incorporated at the overhang created by the enzyme, which can then be quantified to determine the methylation level. This technique relies on efficient restriction digestion of the DNA, is low-throughput, and requires >1 µg of template DNA, which may not be available. Genome-wide changes to DNA methylation can also be investigated using the same techniques that are used for assessing single gene loci methylation. MSP, COBRA,

Sanger sequencing and pyrosequencing are used to determine the methylation status of repeat elements such as LINE1 (see Section 1.3.4), as a surrogate marker of changes to CpG methylation that are occurring across the genome, based on the fact that these elements are heavily methylated.

A recent report found that depending on the method used, different methylation data can be obtained for the same samples, particularly if the study is longitudinal and involves repeat sampling (Wu *et al.*, 2012). Therefore, careful consideration needs to be taken to determine the most appropriate method for determining methylation status, taking into account sample size, the amount of DNA available for analysis, as well as the expected changes in methylation i.e. complete demethylation/methylation vs. small changes at some CpGs; equipment and processing time.

1.3.3 Telomeres and genomic stability

The guanine-rich repeated sequences of DNA at the end of chromosomes are called telomeres, and consist of (TTAGGG) n repeated sequences. Telomeres serve to prevent degradation of the chromosome ends and to prevent fusion of chromosomes. The G-rich DNA strand (termed the G-strand) loops and is stabilised by telomere binding proteins TRF-1 and TRF-2 to form a physical structure at the end of the chromosome, called a “cap” (Figure 1-10). During replication, the enzyme telomerase replaces the telomere repeat sequence. Despite this dedicated enzyme, telomere lengths have been shown to become shorter with each round of cell division. Telomerase preferentially lengthens the shortest telomeres, leading to the

observation of varying telomere lengths within individuals and between individuals. In animal studies, telomere lengths have also been shown to vary depending on the age and sex of the animal and the tissue investigated (Cherif *et al.*, 2003). DNA methylation has also been linked with stable telomere length, where a loss of DNMT1 has been shown to reduce the methylation of the sequences immediately up-stream of the telomere hexamer repeat sequence (known as the sub-telomeric region), and results in shorter telomeres (Ng *et al.*, 2009). However, it has also been reported that a loss of DNMT1 can result in increased telomere length (Gonzalo *et al.*, 2006). Both these studies indicate that the altered DNA methylation of the sub-telomeric region results in altered maintenance of telomeres. Furthermore, it has been demonstrated that altered telomere length can result in increased radiation sensitivity (Goytisolo *et al.*, 2000; Wong *et al.*, 2000; Masutomi *et al.*, 2005). It has been hypothesised that the increased radiosensitivity that is observed in ageing animals may be partly due to reduced telomere length (Drissi *et al.*, 2011). Supporting the connection between altered telomere lengths and radiosensitivity is the observation that the radio-sensitive BALB/c mice have “uncapped” telomeres (Williams *et al.*, 2009).

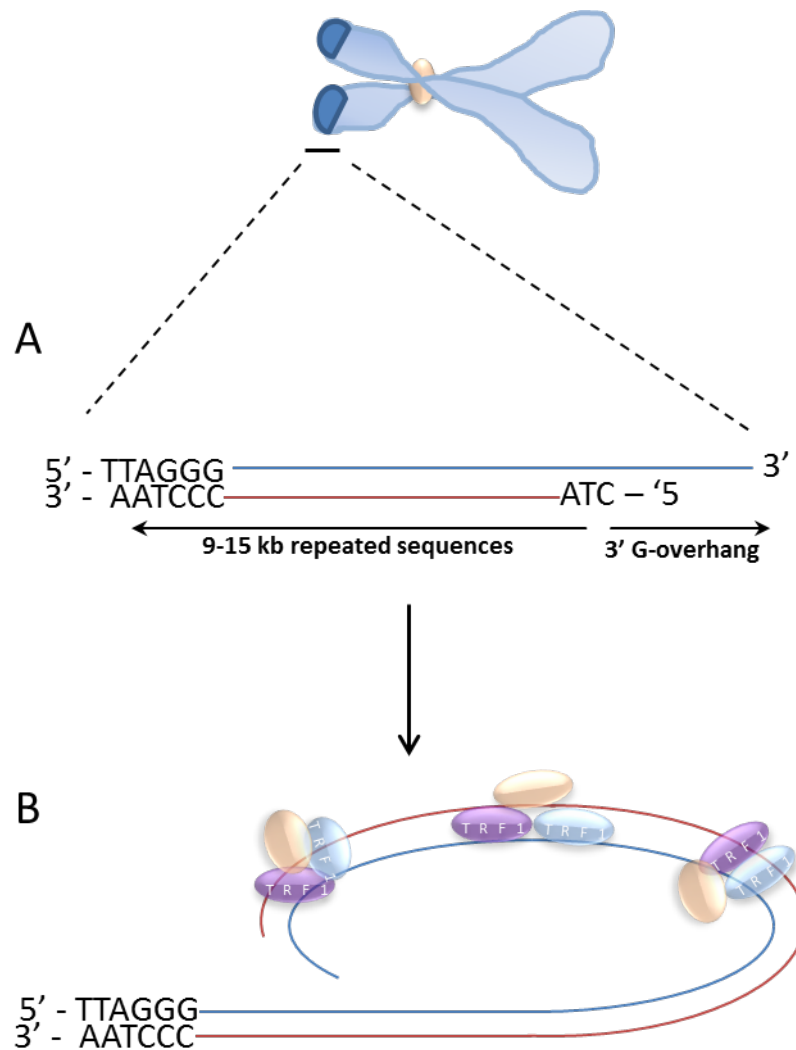


Figure 1-10: Structure of telomeres.

The repeated sequences of DNA at the end of chromosomes are known as telomeres. Telomeres consist of 9-15 kb TTAGGG repeats, with a G-rich leading strand (blue) and a C-rich lagging strand (red). (A) The G-strand (blue) extends in the 3' direction, forming the G-overhang. (B) The G-strand loops and binds to telomere binding proteins TRF-1 and TRF-2 which recruit other proteins to stabilise the telomere. Adapted from O'Sullivan and Karlseder (2010). Shown is the structure of a human telomere.

1.3.4 Retrotransposons and genomic stability

Retrotransposons are essentially parasitic sequences of DNA that through evolution have inserted into the eukaryotic genome. This evolutionary retrotransposition (the ability to change its position within the genome) has created sequence diversity through the creation of new mutations. Transposable elements include Long Interspersed Nucleotide Elements (LINE; L1), Short Interspersed Nucleotide Elements (SINE, Alu, B1) and Long Terminal Repeat elements (LTR) (such as the Intracisternal-A-Particle) (Figure 1-11) (Ostertag, 2001; McCarthy and McDonald, 2004; Farkash and Prak, 2006; Fedorov, 2009). Transposable elements can be described as autonomous or non-autonomous. Autonomous retrotransposons contain machinery necessary for mobility and are able to insert into other regions of the genome. Autonomous retrotransposons include LINE1 and LTR (IAP). Non-autonomous elements include SINE elements (Alu in humans, B1 in mice), and require LINE1 machinery to move across the genome.

The majority of the retrotransposons in the genome contain mutations and truncations that have rendered them incapable of transposition, however it has become evident that there are actively transposing elements within the human and murine genomes. Faulkner *et al* (2009) investigated L1 transcripts in the murine genome and found that 6-30% of mouse RNA transcripts initiate within repeat elements. Of the non-transposon transcripts from the murine genome, 18% had transcription start sites that occurred within repeat elements, and only ~5% of those transcription start sites were retrotransposons. Furthermore, it was evident that the transcription of the L1 elements varied between cell and tissue types, and

that the expression of different L1 families was also associated with cell and tissue type.

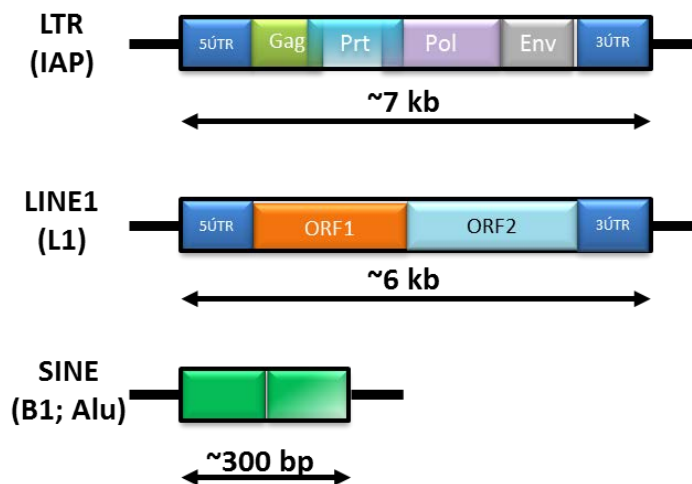


Figure 1-11: Types of retrotransposons.

The types of retrotransposons found in the genome: Long terminal repeat (LTR) elements such as the murine Intracisternal-A-Particle (IAP). These elements consist of long terminal repeat elements in the 5' and 3' UTR, and sequences encoding proteins involved in their autonomous transcription and retrotransposition. The autonomous Long Interspersed Nucleotide Elements (LINE1, L1) consist of a 5' and 3' UTR and open reading frames (ORF) encoding RNA binding proteins and an endonuclease. The non-autonomous Short Interspersed Nucleotide Elements (SINE1), B1 elements in the murine genome and Alu elements in the human genome, require the L1 proteins for transposition, and consist of two monomeric repeats. Adapted from Ostertag (2001).

L1 elements consist of a 5' and 3' UTR, two open reading frames, ORF1 and ORF2, and are ~6 kb in length. Transcripts of L1 elements have been found to consist of either ORF1 and 2 or just ORF2. A full-length L1 element is transcribed from its internal promoter to produce mRNA (Figure 1-12a). The RNA moves to the cytoplasm where ORF1 and ORF2 proteins (ORF1p and ORF2p) are translated. ORF1p is an RNA binding protein and is involved in the movement of the mRNA back into the nucleus, while ORF2p is an endonuclease. Following translation, a ribonucleoprotein complex forms between the RNA, an ORF2 and one or more

ORF1 proteins (Figure 1-12b). This complex is an intermediate to retrotransposition. The L1 ORF2p nicks DNA in a target site, creating a 3'OH (hydroxyl) overhang. The mRNA binds to the nicked DNA and reverse transcription takes place from the 3'OH overhang (Figure 1-12c-d). The newly synthesised cDNA is integrated into the DNA, following which the second strand is synthesised, creating a new L1 copy (Figure 1-12e-f). This process is known as target-primed reverse transcription and utilises the "host" cell's own transcriptional machinery. The SINE elements (human Alu and murine B1) are shorter repeat elements of approximately 300 bp. Despite being shorter than L1 elements, and lacking the proteins to actively transcribe and transpose, Alu/B1 elements are prevalent throughout the mammalian genome and show recent evolutionary insertions (reviewed in Batzer and Deininger, 2002; Akagi *et al.*, 2008). Alu/B1 element mobilisation appears to occur using the L1 ORF1 and 2 proteins for retrotransposition, as the sequence in the target site is flanked by target site sequence duplications that have close similarity to L1 target site duplications. Furthermore, the 5'UTR region of the Alu/B1 have been found to contain the ORF2p sequence motif (de Andrade *et al.*, 2011). The IAP Long Terminal Repeat element (IAP_LTR) is described as an endogenous retrovirus. It contains overlapping open-reading frames (ORFs) for a group-specific antigen (Gag), protease (Prt), polymerase (Pol), and terminal LTRs. The Pol genes encode a reverse transcriptase, ribonuclease H, and integrase to generate proviral complementary DNA (cDNA) from viral genomic RNA to insert into the target site. Following transcription, mRNA is moved to the cytoplasm where the particle proteins are translated (Figure 1-13a-b). Reverse transcription of the mRNA occurs in the cytoplasm following which the proviral cDNA is shuttled into the nucleus (Figure

1-13c). The IAP DNA is then incorporated into the target site via integrase, creating a new IAP copy (Figure 1-13d-e) (Mietz *et al.*, 1987; Kuff and Lueders, 1988; Gaubatz *et al.*, 1991; Dewannieux *et al.*, 2004).

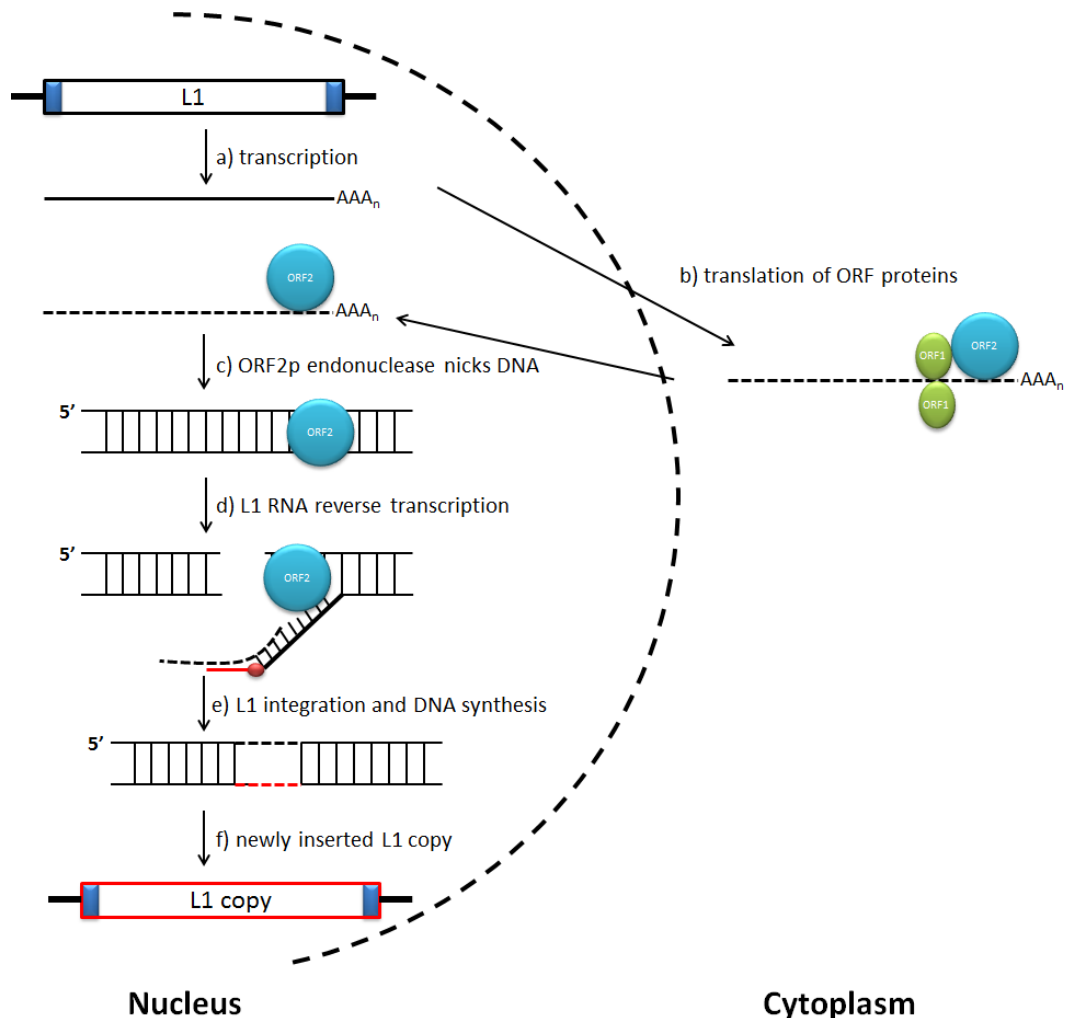


Figure 1-12: L1 transcription and retrotransposition.

(A) A full length L1 mRNA (solid line with poly-A tail) is transcribed from its promoter and moves to the cytoplasm. The L1 open reading frame (ORF) 1 and 2 proteins are translated (B), following which a ribonucleoprotein complex is formed between the mRNA (dotted line with poly-A tail), one ORF2p (blue circle) and one or more ORF1p (green circle). (C) The complex moves into the nucleus where the ORF2p, which is an endonuclease, nicks one DNA strand in a target site creating a 3'OH overhang (red circle). (D) The L1 mRNA binds to the nicked DNA strand following which reverse transcription takes place using the 3'OH as a priming site to produce L1 cDNA (solid red line). (E) The ORF2p endonuclease then nicks the other DNA strand and the L1 is integrated into the target site. (F) DNA synthesis occurs to produce a newly inserted L1 copy. Adapted from Ostertag (2001).

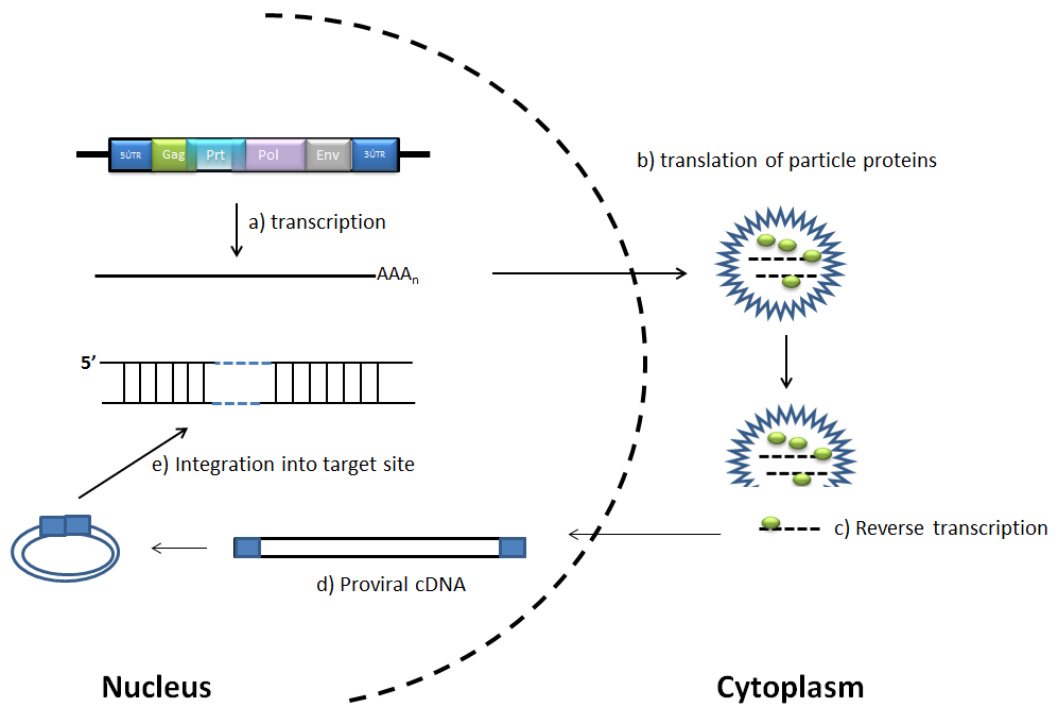


Figure 1-13: IAP transcription and retrotransposition.

(A) IAP mRNA (solid line with poly-A tail) is transcribed from its promoter and moves to the cytoplasm. (B) Translation of the particle proteins occurs, following which the IAP mRNA is reverse transcribed to proviral cDNA (dotted line) and (C) shuttled to the nucleus. (D) Proviral DNA is synthesised (box and circle) and (E) integrated into the target site via integrase (dotted blue line). Adapted from Koito and Iketa (2012).

Retrotransposons are located predominantly in heterochromatin and are associated with high CpG methylation and repressive histone marks, including histone H3 (lysine) K9, K27 and K20 tri-methylation (Martens *et al.*, 2005). However, recent studies have demonstrated that the repeat elements can be found upstream of coding genes and have been found to influence, and in some cases, control the expression of the genes. A well-known example is the A^{VY} allele. The *Agouti* gene encodes fur coat colour phenotype in mice. Normal *Agouti* expression results in a brown (pseudoagouti) phenotype. However, it has been found that there is an IAP element inserted upstream of the *Agouti* gene. Active transcription from the IAP 5'UTR promoter produces an alternate transcript which results in the A^{VY}

phenotype. Due to mosaic expression of A^{vy} , mice vary from agouti/yellow to pseudoagouti, but can also be mottled in appearance (Morgan *et al.*, 1999). Silencing of the IAP transcript upstream of *Agouti* has been demonstrated to be due to CpG methylation of the 5'UTR, and supplementation with a dietary methyl donor can produce offspring that shift from agouti to pseudoagouti compared with dams (Wolff *et al.*, 1998; Cooney *et al.*, 2002; Cropley *et al.*, 2010).

It is well documented that DNA damaging agents can induce a reduction in methylation of CpGs located within the promoters of the repeat elements and can result in increased transcript levels. Chemotherapeutic agents such as Etoposide, which induce double strand breaks and inhibit repair, and 5-aza-2'-deoxycytidine, an analogue of cytosine that cannot be methylated (Rudin and Thompson, 2001; Hagan *et al.*, 2003) both induce hypomethylation. Other examples of DNA damaging agents are chemicals used to manufacture plastics such as Bisphenol A (Dolinoy *et al.*, 2007), and particulate air pollution (Baccarelli *et al.*, 2009). Hypomethylation of the repeat element promoters has also been shown to occur following irradiation (Giotopoulos *et al.*, 2006; Filkowski *et al.*, 2010), and in some reports this has resulted in an increase in L1 and IAP transcripts (Faure *et al.*, 1997; Farkash *et al.*, 2006). However, in several reports, following irradiation, an increase in L1 methylation has also been observed (Kaup *et al.*, 2006; Kongruttanachok *et al.*, 2010; Aypar *et al.*, 2011; Goetz *et al.*, 2011). Hypomethylation of these elements also occurs with ageing (Barbot *et al.*, 2002; Bollati *et al.*, 2009; Jintaridith and

Mutirangura, 2010), cancer (Howard *et al.*, 2007; Ogino *et al.*, 2008a; 2008b; Irahara *et al.*, 2010), and in developmental defects (Wang *et al.*, 2010).

1.4 DNA methylation and radiation exposure

There is only one published report examining the effect of ionising radiation on promoter CpG methylation at individual loci, where investigators assessed the methylation levels of the tumour suppressor gene p16^{INKa} and the DNA repair gene O⁶-methylguanine-DNA methyltransferase (MGMT)(Kovalchuk *et al.*, 2004a). Nearly all studies investigating the effect of ionising radiation on DNA methylation levels have focussed on global DNA methylation levels. Kalinich *et al* (1989) were the first to demonstrate a dose dependent decrease in total (global) 5mdC content in cell lines following irradiation with 0.5 - 10 Gy. Subsequent *in vitro* studies have demonstrated variable methylation responses following HDR exposure including hyper- and hypomethylation, as well as no alteration in methylation levels (Kaup *et al.*, 2006; Kongruttanachok *et al.*, 2010; Aypar *et al.*, 2011; Goetz *et al.*, 2011; Armstrong *et al.*, 2012). *In vivo* studies have also shown variable responses of murine 5mdC levels following irradiation. Tawa *et al* (1998) demonstrated that radiation doses ranging from 4-10 Gy induced a loss of methylation in murine liver. Other mouse studies have demonstrated that there are tissue and sex differences in genomic DNA methylation levels following irradiation, as well as the timing of analysis. A summary of the published *in vivo* DNA methylation studies using ionising radiation is presented in Table 4. Of particular note are the differences in radiation dose, dose-rate, timing post-irradiation and the tissues investigated between the

studies. For example, a study conducted by Kovalchuk *et al* (2004a) demonstrated the importance of timing when 2 h following irradiation with 0.5 Gy at a low dose-rate (2 mGy/s) did not induce any changes in the liver or muscle tissues of irradiated mice, however a chronic irradiation at the same dose-rate resulting in an accumulated exposure of 0.5 Gy, induced a loss of methylation in muscle tissue.

The experiments presented in Table 4 have been performed in C57Bl/6 mice, which are considered to be radioresistant. One study has been conducted to determine if there is disparity in the modulation of DNA methylation between radioresistant (C57Bl/6) and radiosensitive (CBA) mice (Giotopoulos *et al.*, 2006). This study observed that at 4 days following irradiation with 3 Gy, there was a persistent loss of methylation in the bone marrow of the CBA mice, which was also observed in mice at 42 days post-irradiation. No effect was observed in the bone marrow of the C57Bl/6 mice, and spleen tissues from both strains did not demonstrate a loss of methylation at any time-point investigated. This evidence suggests that the mechanisms that contribute to the radiation-sensitivity of the CBA mice, as determined by time to lethality, tumour formation and overall genomic instability may involve the modulation of DNA methylation and are tissue-dependent.

Table 4: Summary of published *in vivo* murine DNA methylation and ionising radiation studies.

Mouse Strain	Sex	Dose	Dose Rate	Time Post-Irradiation	Tissue	Change to	Author	
						Methylation Levels		
C57Bl/6	unknown	4, 7, 10 Gy	0.27 Gy/min	24, 48, 72 hours	spleen	n/c	Tawa <i>et al</i> , 1998	
					liver	↓		
					brain	n/c		
	male and female	acute 0.5 Gy	2 mGy/s	2 hours		liver	n/c	Kovalchuk <i>et al</i> , 2004
						muscle	n/c	
	chronic 0.5 Gy	50 mGy/day (2 mGy/s)	daily for 10 days; 2 hours following last irradiation		liver	n/c		
					muscle	↓ (males)		
	male and female	0.5, 1, 2.5, 5 Gy	5 Gy/min	6 hours	spleen	↓	Pogribny <i>et al</i> , 2004	
					liver	↓ (males)		
		4 weeks	spleen	n/c				
			liver	n/c				
		5 Gy	0.5 Gy/min	6 hours	spleen	↓		
					liver	↓ (females)		
	4 weeks	spleen	n/c					
		liver	n/c					
male and female	acute 0.5 Gy	2 mGy/s	3 hours	liver	n/c	Raiche <i>et al</i> , 2004		
				spleen	↑ (males)			
	chronic 0.5 Gy	50 mGy/day (2 mGy/s)	daily for 10 days; 2 hours following last irradiation	liver	↓ (females)			
				spleen	↓ (females) ↑ (males)			
male and female	5 Gy	5 Gy/min	6 hours	thymus	↓	Koturbash <i>et al</i> , 2005		
				muscle	↓			
	4 weeks	thymus	↓					
		muscle	n/c					
	5 Gy	0.5 Gy/min	6 hours	thymus	↓			
				muscle	n/c			
	4 weeks	thymus	↓ (males)					
		muscle	n/c					
male and female	acute 0.5 Gy	2 mGy/s	3 hours	thymus	↓	Pogribny <i>et al</i> , 2005		
	chronic 0.5 Gy	50 mGy/day (2 mGy/s)	daily for 10 days; 2 hours following last irradiation	thymus	↓			
CBA	unknown	3 Gy	0.5 Gy/min	4-42 days	BM	n/c	Giotopolous <i>et al</i> , 2006	
					spleen	n/c		
					BM	↓		
					spleen	n/c		
C57Bl/6	male	2.5 Gy	3 Gy/min	4 days	testes	↓	Fillowski <i>et al</i> , 2010	

n/c – no change

↑ - increase in methylation levels; ↓ - decrease in methylation levels

DNA methylation plays an important role in establishing gene expression patterns during development. Hence, the disruption of germline DNA methylation patterns may affect the genome stability of offspring. The effect of radiation on global DNA methylation levels in the germline has also been investigated (Table 5). Koturbash *et al* (2006) reported that offspring of C57Bl/6 mice irradiated with a whole body

dose of 2.5 Gy and mated one week following exposure, had reduced methylation levels in the thymus, but not in spleen or liver tissues. This has also been observed for the methylation of repetitive elements, where a decrease was detected in the thymus of offspring following paternal irradiation with 2.5 Gy (Filkowski *et al.*, 2010).

Table 5: Summary of published *in vivo* transgenerational murine DNA methylation and ionising radiation studies.

<i>Mouse Strain</i>	<i>Sex of irradiated parent</i>	<i>Dose</i>	<i>Dose-Rate</i>	<i>Age of progeny</i>	<i>Tissue</i>	<i>Change to Methylation Levels</i>	<i>Author</i>
C57Bl/6	male and female	2.5 Gy	unknown	15 days	spleen	n/c	Koturbash <i>et al.</i> , 2006
					liver	n/c	
					thymus	↓	
	male	2.5 Gy	3 Gy/min	6 months	thymus	↓	Filkowski <i>et al.</i> , 2010

↑ - increase in methylation levels; ↓ - decrease in methylation levels
n/c – no change

In some of the experiments found in Table 4, the loss of methylation can be attributed to a failure of maintenance methylation. Following chronic irradiation with 50 mGy/ day for ten days, it was shown that there were reduced levels of the maintenance methyltransferase, DNMT1. This loss of DNMT1 was also associated with an increase in the accumulation of γ -H2AX foci, indicating an association between a reduction in methylation and DNA DSBs (Pogribny *et al.*, 2005). Furthermore, there were reduced levels of the *de novo* methyltransferases DNMT3a/b, methyl-binding proteins implicated in chromatin compaction, as well as reduced tri-methylation of histone H4-Lys20. Tri-methylation of histone H4 is associated with transcriptionally active heterochromatic regions of DNA that are

generally CpG rich, heavily methylated and contain repetitive elements. Declining heterochromatin DNA methylation and histone H4-Lys20 methylation levels have been associated with both cancer and ageing (Fraga *et al.*, 2005).

Taken together, the few *in vivo* DNA methylation and radiation exposure studies that have been conducted indicate that very little is known about DNA methylation responses following irradiation, in particular the temporal and tissue-specific effects of the radiation-induced modulation and how this contributes to radiation-induced genomic instability and carcinogenesis.

1.5 Aims of this thesis

The modulation of DNA methylation, both genomic 5mC levels and repeat element methylation, has been shown to be affected by exogenous and endogenous factors which can result in increased genomic instability. The studies described in this thesis aimed to investigate repeat element methylation modulation *in vivo* following X-irradiation. The first aim of this thesis was to develop a sensitive, high throughput screening assay that was able to detect changes in methylation of L1 repeat elements. This assay was then used to investigate the temporal modulation of L1 repeat element DNA methylation in three strains of laboratory mice that differ in their radiosensitivity. It was hypothesised that the more radiosensitive mouse strains would elicit greater and more persistent modulation of repeat element DNA methylation. The assay was also used to monitor changes in peripheral blood L1 DNA methylation levels longitudinally in ageing mice that had been exposed to low dose X-radiation, with the hypothesis that the adaptive response would reduce, or prevent the decline in DNA methylation in ageing animals. Overall, the studies in this thesis sought to further understand the role that the modulation of DNA methylation plays in radiation-induced genomic instability by investigating the methylation levels of repeated sequences of DNA, whose demethylation has been implicated in increased genomic instability.